

The Nile deep-sea fan: An example of interacting sedimentation, salt tectonics, and inherited subsalt paleotopographic features

Lies Loncke^{a,*}, Virginie Gaullier^b, Jean Mascle^c, Bruno Vendeville^d, Laurent Camera^c

^a *Département de Géologie, UMR 8110, Université de Picardie Jules Verne, 33 rue de Saint Leu, 80039 Amiens, France*

^b *Université de Perpignan, LEGEM, 52 avenue Paul Alduy, 66860 Perpignan, France*

^c *Géosciences Azur, BP 48, 06235 Villefranche-sur-mer, France*

^d *UMR 8110, Bâtiment SN 5, Université de Lille1, 59655 Villeneuve d'Ascq, France*

Received 4 July 2005; received in revised form 5 January 2006; accepted 21 January 2006

Abstract

Structural analysis of the Nile deep-sea fan (NDSF) indicates that post-Miocene deformation is largely controlled by down-slope movement above a Messinian salt layer. In contrast to other similar systems, the NDSF shows significant lateral asymmetry, and three distinct provinces can be recognized. Regional variations in salt thickness and base-salt geometry within the system have led to the presence of structures typical of both gravity gliding and gravity spreading. Trends of structures within the western and central parts of the NDSF are consistent with forming due to gravity gliding processes. This pattern contrasts with that in the eastern NDSF that seem to be much more consistent with deformation due to gravity spreading. Observed differences in structural style across the NDSF can be related directly to the paleomorphological evolution of the Nile cone during Messinian time, which is perhaps partly related to features that have been inherited from early Mesozoic evolution of the North Egypt passive margin. In the east part of the NDSF, the structural evolution has been significantly influenced by the proximity of Eratosthenes Seamount. This large topographic buttress has served to both limit and deflect northeastward allochthonous advance of the Messinian evaporites and has thus severely complicated deformation of the overlying Plio-Quaternary sedimentary cover within the broad corridor that runs NNW–SSE and cuts obliquely across the modern bathymetry of the Nile cone.

© 2006 Elsevier Ltd. All rights reserved.

Keywords: Salt tectonics; Deep-sea fan; Inheritance

1. Introduction

1.1. Overview of structural styles on salt-bearing passive margins

Salt-bearing passive continental margins display a great variety of structures related to thin-skinned, gravity-driven salt tectonics and are, in essence, areas of mechanical decoupling between the subsalt sedimentary ‘basement’, the salt layer, and its sedimentary overburden (Diegel et al., 1995; Rowan et al., 1999; Trudgill et al., 1999; Cramez and Jackson, 2000; Stover et al., 2001). In such settings, loading of a weak, viscous, and mobile evaporitic layer by wedges of sediments triggers overall seaward spreading and/or gliding of both the salt layer and its overburden. Gravity spreading and gliding are both

characterized by proximal thin-skinned extension on the shelf and the upper continental slope and by distal contraction on and in front of the lower slope (Vendeville, 2005). Generally, proximal extension is expressed by ductile thinning of the evaporitic salt layer and faulting of the brittle sedimentary overburden. There, listric normal growth faults or shallow grabens can trigger the reactive rise of underlying diapiric salt ridges (Vendeville and Jackson, 1992a,b). In map view, grabens and associated reactive diapirs can have arcuate traces and bound subcircular or polygonal minibasins (Diegel et al., 1995; Rowan et al., 1999). Distal thin-skinned contraction causes thickening of the salt layer and, sometimes, seaward spreading of a salt nappe, beyond its original deposition limit. Typically the distal edge of an advancing salt nappe is marked by an abrupt scarp on the seafloor, as illustrated by the Sigsbee nappe in the deep-water Gulf of Mexico (Diegel et al., 1995; Rowan et al., 1999). In the brittle overburden, shortening is accommodated by the formation of buckle folds and reverse faults.

Although gravity gliding and spreading are characterized by the same three structural domains (extension/translation/contraction), they have different triggering mechanisms and

* Corresponding author. Tel.: +33 32282 76 39; fax: +33 3 22 82 75 76.
E-mail address: lies.loncke@u-picardie.fr (L. Loncke).

generate different structural styles. Downslope gliding takes place when the base of the salt layer and the top of the overburden dip seaward. Gliding is accommodated by normal faults in the proximal region and by contractional folds or faults in the distal region (Vendeville and Cobbold, 1987). Because the base-salt slope is controlled by large-scale processes (thermal or tectonic subsidence), basal slope orientation and the direction of gravity gliding vary only moderately along local segments of a margin. Therefore, the traces of normal faults forming during gravity gliding tend to be subparallel.

Gravity spreading prevails where the base of the salt layer is nearly horizontal or even slightly tilted landward (e.g. above a crustal flexure formed in response to sediment loading). The forces driving gravity spreading result from the slope of the top of the overburden (i.e. the bathymetric slope). Typically, the sedimentary strata in deep-sea fans thin seaward, resulting in an overall seaward-facing wedge and seaward-dipping seafloor. Lateral thickness changes with such a wedge induce lateral gradients in lithostatic stresses, thus generating the gravity instability driving spontaneous seaward spreading of the sediment wedge above the mobile substrate (Vendeville, 2005). Spreading of the salt and its sedimentary overburden is approximately parallel to the direction of the local bathymetric slope. Unlike processes controlling the basal slope (regional subsidence), the local surface slope may vary greatly at the subregional or even local scale. Where the surface slope is simple, traces of proximal normal faults are all parallel and sublinear (generally parallel to the coastline). Where local slope directions diverge or converge, several sets of normal faults having multidirectional traces form (Cobbold and Szatmari, 1991; Gaullier and Vendeville, 2005). Gravity spreading appears, therefore, to be a process capable of creating polygonal minibasins (Rowan et al., 1999; Gaullier and Vendeville, 2005).

In summary, the balance between gravity gliding and spreading determines the structural style of salt tectonics. Where gravity gliding dominates, structures tend to be cylindrical and perpendicular to the regional basal slope direction. They can be readily studied on 2D seismic surveys. Where gravity spreading dominates, the presence of radial and concentric extensional structures, along with polygonal and subcircular depocenters, makes any structural analysis far more challenging.

Furthermore, complexity of the structural patterns created by gravity gliding or spreading can increase if the area is subjected later to tectonic superimposition of phases of shortening or strike-slip. For example, Cramez and Jackson (2000) described how depocenters that formed initially by raft tectonics (extension) were later reactivated in compression. Likewise, Nilsen et al. (1995) and Vendeville and Nilsen (1995) demonstrated that tectonic (i.e. crustal-scale) extension or shortening deformed and reactivated a network of depocenters and diapirs in the Nordkapp Basin, Norway. One last feature capable of further complicating structural outcome is the presence of inherited subsalt basement structures, such as syn-rift normal or transform faults. One such example has been

described in the Gulf of Lions by Gaullier (1993), Gaullier and Bellaiche (1996), and Maillard et al. (2003). Subsalt basement faults, even if they are no longer active during gravity gliding or spreading can influence rates of downslope translation because they cause abrupt changes in salt thickness across paleo-fault scarps. As such, they may induce local shortening, extension, or strike-slip movement of the sedimentary overburden.

1.2. Goals of the study

Prior to 1998, little was known about the Nile deep-sea fan (NDSF). Since then, several geological–geophysical surveys have been carried out mainly by the Géosciences Azur laboratory ('Primed II', 'Fanil', and 'Medisis' surveys, completed in 1998, 2000 and 2002, respectively). During these operations, multibeam swath bathymetry, acoustic imagery (Simrad/EM12 and EM300 echo-sounders), 6-channel-high speed, 24-channel-high resolution seismic reflection profiles and multichannel reflection data were acquired. For the first time, the NDSF has thus been nearly entirely mapped (Fig. 1). A preliminary analysis of this data set emphasized the importance of salt tectonics in the structural style of this turbiditic system (Gaullier et al., 2000). Even though the deep-sea fan appears to have been shaped mainly by gravity-driven salt tectonics, it also shows morphological characteristics that may be related to deep-seated, crustal-scale tectonics (Masclé et al., 2000). For example, in the eastern province of the NDSF, there is an actively deforming corridor more than 250 km long and trending NNW–SSE that obliquely intersects the continental slope (Fig. 1). The origin of this corridor is still debated and could represent the offshore prolongation of the Suez rift (Masclé et al., 2000). Alternatively, this corridor could have been formed by gravity-driven salt tectonics alone (Gaullier et al., 2000). Finally, this corridor could result from a combination of both gravity-driven, thin-skinned, and crustal scale, thick-skinned, tectonics.

On the basis of seismic and swath bathymetry data (Loncke et al., 2002b), we propose a comprehensive synthetic interpretation of the NDSF structure and its evolution since Messinian times. We restrict our study to the Messinian and post-Messinian NDSF because (1) the Plio-Quaternary NDSF is structurally decoupled by Messinian evaporites from its pre-Messinian sedimentary basement and (2) seismic penetration is generally poor below the Messinian salt, at least on the six-channel seismic data we acquired. An analysis of the deep structures of the area, based on multi-channel seismic and gravity data, is presently carried out (Masclé et al., 2003).

2. Egyptian margin: geological background

2.1. Tectonic framework

The Nile deep-sea fan (NDSF) forms a thick sedimentary wedge covering about 100,000 km², constructed, for the most part, since the late Miocene by influx of clastic sediments from

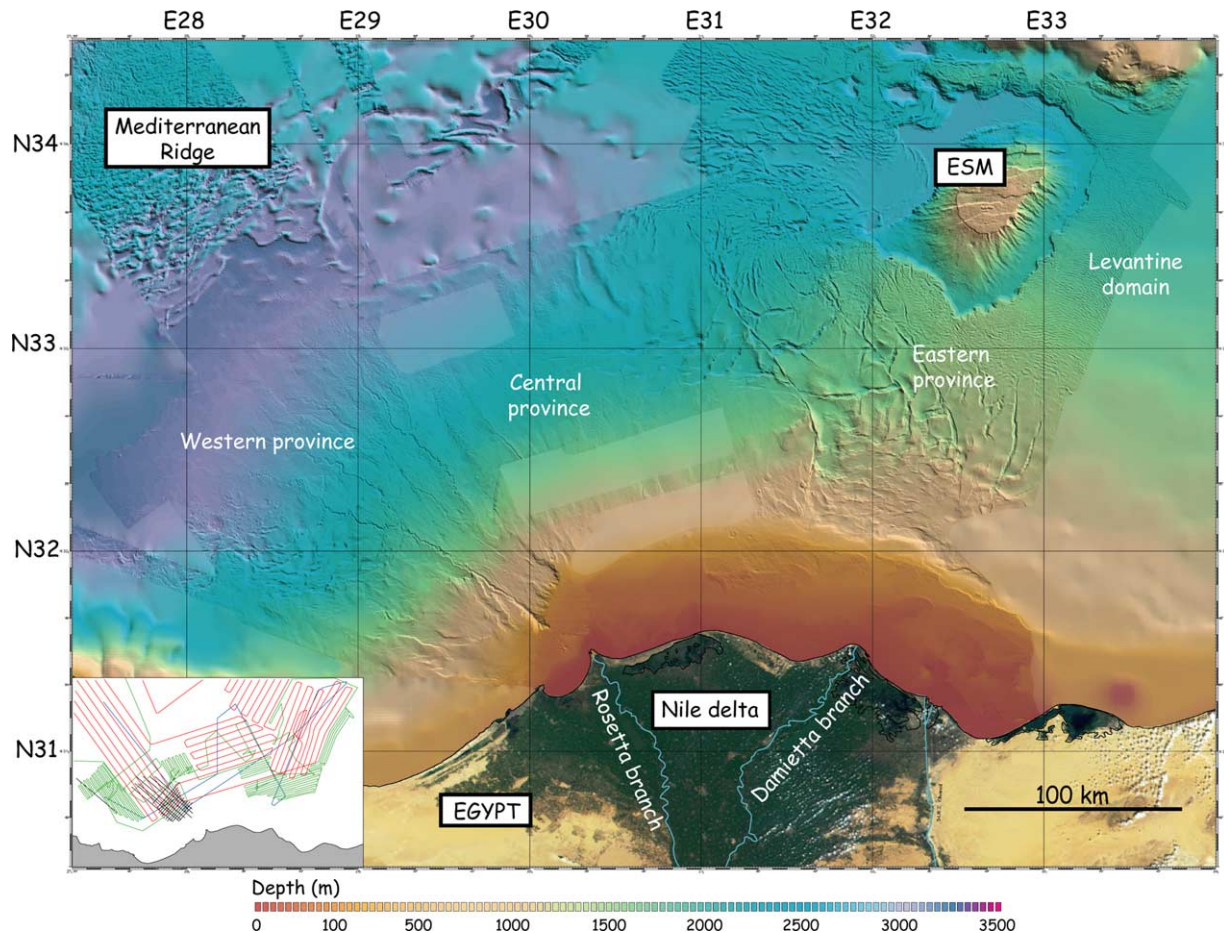


Fig. 1. Shaded bathymetric map of the Nile deep-sea fan (from combined EM12, EM300, and ICBM data). Bottom-left inset indicates tracklines of surveys (prised II in red, Fanil in green, Médisis in blue, and BP-Egypt in black). Note the sharp morphological contrasts between west, central, and east provinces (see text for details) (for interpretation of the references to colour in this figure legend, the reader is referred to the web version of this article).

the Nile River (Salem, 1976; Dolson et al., 2000). The present-day NDSF covers a segment of an older passive margin thought to have formed during successive rifting episodes in Jurassic and early Cretaceous times (Biju-Duval et al., 1978; Morelli, 1978; Hirsch et al., 1995). According to Aal et al. (2001) and Mascle et al. (2003), the total thickness of sediments on the Egyptian margin (including the post-Miocene NDSF) could exceed 9 km.

The geodynamic framework of the eastern Mediterranean and its surroundings is characterized by a complex pattern of active, thick-skinned, crustal-scale tectonics (McKenzie, 1972; Neev, 1975; Courtillot et al., 1987; Sage and Letouzey, 1990; Le Pichon et al., 1995; Mascle et al., 2000; McClusky et al., 2000), resulting from interactions between various tectonic plates and microplates (Fig. 2). Geodynamic features surrounding the region are (a) in the southeast, the almost-aborted Suez Rift; (b) in the east and northeast, the Dead Sea/Levant and East Anatolian Fault zones related to the motion of the Arabian plate with respect to Africa; (c) northward, along the eastern Hellenic and Cyprus arcs, the subduction/collision of Africa beneath Europe and the rapidly moving Aegean–Anatolian microplate (Sage and Letouzey, 1990; Chaumillon et al., 1996; Huguenot, 2001); and (d) the Egyptian margin, a passive margin of Mesozoic age that may have been reactivated partly during

Miocene rifting of the Suez–Red Sea Rift system (Guiraud and Bosworth, 1999; Mascle et al., 2000). In this tectonic framework, sediments of the NDSF drape onto the former Egyptian passive margin and reach north to the subducting Tethyan oceanic domain. The distal parts of the NDSF, however, have not yet reached the Hellenic and Cyprus arcs: its western edge feeds the accretionary Mediterranean Ridge (MR), whereas its eastern corner is bounded by an almost flat-topped, subcircular seamount (Eratosthenes Seamount, hereafter referred to as ‘ESM’). This bathymetric high is interpreted to have a continental origin, having been rifted away from the African/Levant domain during the Mesozoic. It is currently colliding against the island of Cyprus (Robertson et al., 1995; Guiraud and Bosworth, 1999). According to Abdel Aal et al. (2000) and Samuel et al. (2003), two major fault trends characterize the offshore NDSF. The Tamsah trend (oriented NW–SE) and the Rosetta trend (oriented NE–SW to ENE–WSW) are both thought to be inherited from the Mesozoic rifting phase.

Superimposed onto an already complex structural framework are the geological consequences of the Messinian (latest Miocene) desiccation event, which led to deposition, in most of the area now occupied by the NDSF, of large quantities of evaporites (Ryan and Hsü, 1973; Sage and Letouzey, 1990).

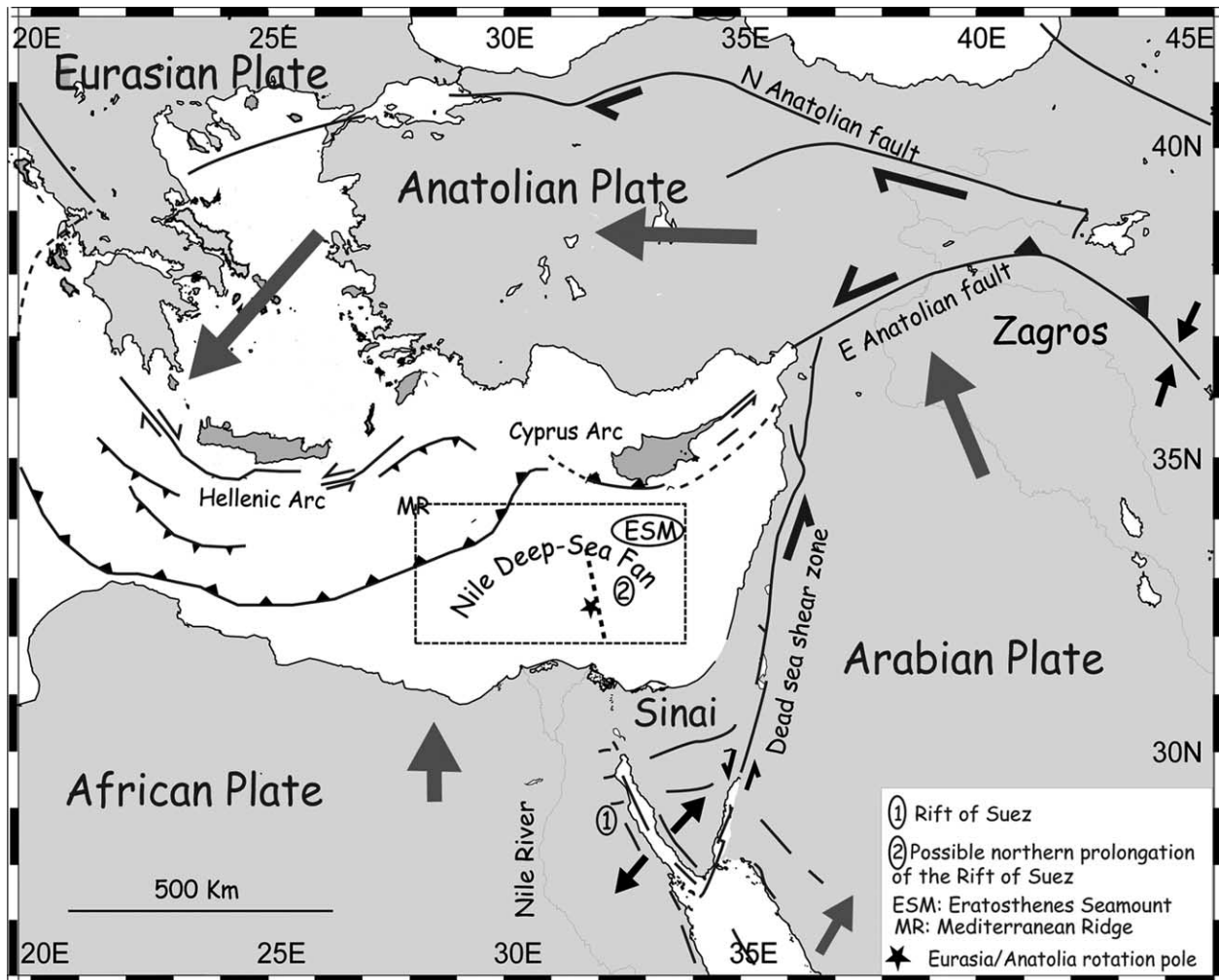


Fig. 2. Geodynamic setting of the Eastern Mediterranean basin. Study area indicated by dotted box. Grey arrows indicate relative plate motions.

Loading of these ductile evaporitic layers under thick Plio-Quaternary sediments later triggered spectacular gravity-driven salt tectonics that continue to the present-day (Ross and Uchupi, 1977; Sage and Letouzey, 1990; Kempler et al., 1996; Gaullier et al., 2000; Loncke, 2002; Loncke and Mascle, 2004). Faults and folds related to salt movement are clearly expressed on bathymetric data across most of the region.

2.2. Seismic stratigraphy from Messinian to Pleistocene

One key to understanding deformation style in the NDSF lies in its stratigraphy. The NDSF's stratigraphy has recorded major sea-level fluctuations, including the huge relative sea-level fall (related to the progressive closing up of the Mediterranean basin) that led, in Messinian times, to the creation of a main erosion surface and to deposition of thick evaporitic layers (mainly halite), forming a regional mobile layer within the sedimentary cover.

Depending on the author, different intervals are defined in the Mediterranean for this event, differences mainly relating to the way the Messinian event is studied (onshore through fieldwork or offshore using seismic data). Some authors (e.g. Rouchy and Saint Martin, 1992) define three sedimentary

facies: (1) the 'lower evaporites' that consist essentially of massive salt layers (halite) and mark the height of the Messinian salinity crisis, (2) the 'upper evaporites', made of a cyclic alternation of marls and gypsum and related to episodic infilling events of the Mediterranean basin, and, finally, (3) the 'lago-mare' facies, corresponding to one widespread lacustrine event that predated the final refilling of the Mediterranean basin. This sea-level fall (estimated to have been at least 1000 m) caused massive erosion of the surrounding continental margins, producing large quantities of clastic detrital deposits before, during, and after salt deposition in the deep basin (Ryan and Hsü, 1973; Lofi, 2002; Lofi et al., 2003). The top and base of the evaporites can generally be identified on seismic profiles (Ryan and Hsü, 1973). However, because the deep-basin evaporites themselves have never been sampled by wells, establishing a reliable seismic stratigraphy is difficult (see Lofi, 2002, and abstracts from the conference The Messinian Crisis Revisited, July 2004, Corte). What marine geologists call the 'lower evaporites' corresponds to a highly reflective series of probably detrital sediments deposited by slumping processes during the first stage of sea-level fall. In the deep basin, above these layers, acoustically transparent layers characterize the mobile evaporites made essentially of halite. The upper

evaporites, appearing as layered and reflective packages above these transparent layers, most likely correspond to cyclic alternations of marls and gypsum, as defined by Rouchy and Saint Martin (1992). The problem is that during the whole salinity crisis, erosion was active on the margin, leading to detrital deposits interfingered between salt and upper evaporites. Although distinguishing transparent salt from reflective detrital rocks is easy, distinguishing upper evaporites from clastic rocks is difficult and greatly depends on the quality of available seismic data. In the case of the NDSF area, the Messinian unconformity is clear, especially below the present-day continental shelf, in an area probably corresponding to wide Messinian badlands (Ryan, 1978). Offshore, Messinian canyons are filled with highly reflective clastic packages referred to as the Abu-Madi Formation (EGPC, 1994; Aal et al., 2000) (Fig. 3). The age of this formation remains controversial (Messinian, Pliocene or both?) and it is made up of a series of thick sand bodies interbedded with shale. At the mouth of the Messinian canyons, some of them up to 1000-m deep, ‘Abu-Madi’ depositional lobes commonly interfinger with the coeval basinward Messinian evaporites. These lobes were deposited in a complex subaerial deltaic/shallow-marine setting, likely forming a ‘proto-cone’ during and after salt deposition (EGPC, 1994). The basinward halite-rich layers are mostly in concordance with pre-Messinian strata and appear acoustically transparent (Fig. 3) or interfinger with coeval, detrital, highly reflective packages (landward). These reflective packages, probably corresponding to upper evaporites or detrital sediments, generally overlay transparent halite layers (Fig. 3). The general pattern in which the Messinian event is

characterized upslope by erosional surfaces and basinward by transparent halite layers is complicated by the presence of ESM that was emergent during sea-level fall. This basinward relief has been peneplained and strongly karstified (Robertson, 1998), explaining the origin of the remarkable flat-topped topography of the seamount. In Pliocene times, after the basin was refilled as a result of the reopening of the Straits of Gibraltar, NDSF sedimentation was dominated by clays and interbedded sands, reflective of an outer-shelf depositional environment (EGPC, 1994). Throughout Pliocene times and especially during Quaternary times, the Messinian salt and associated time-equivalent subaerial deposits have been covered progressively by a large deep-sea fan. In most areas, the Plio-Quaternary cover is characterized by strong-amplitude, layered reflectors typical of turbiditic sedimentation. Buried channel-levee systems are numerous. Some acoustically transparent lenses are also frequently observed, suggesting that slope instability and slumping processes have occurred during the growth of the fan (Loncke, 2002; Loncke et al., 2002a). However, no significant regional seismic reflector can be easily defined or tracked across large distances within the Plio-Quaternary cover, making regional seismic correlation difficult.

3. Data set and methods

The ‘Prismed II’ and ‘FaniI’ surveys, aboard the R.V. ‘l’Atalante’ and ‘Le Suroît’, respectively (in early 1998 and late 2000), provided continuous bathymetric and back-scatter images of the NDSF, using Simrad EM12-Dual

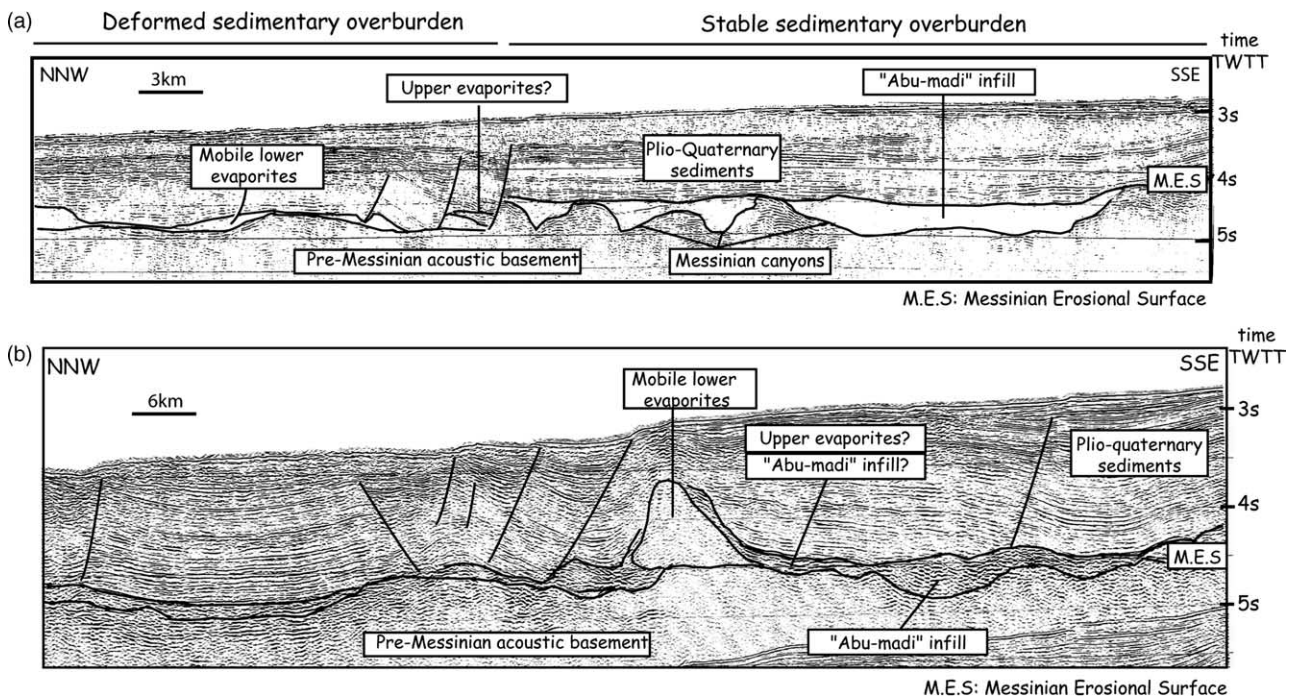


Fig. 3. Seismic-reflection profiles typical of west and central provinces illustrating the stratigraphic characteristics of the area. On profile A, note that Plio-Quaternary sediments are stable where they overlie Messinian canyons, whereas they are deformed where they were deposited on seismically transparent, mobile, lower evaporites. Profile B illustrates how the Messinian Erosional Surface (MES) is overlain by either highly reflective packages infilling the canyons (Abu-Madi) or seismically transparent, lower evaporites forming diapirs.

and EM300-Dual multibeam sounding systems (Fig. 1). The Simrad EM12-Dual system records along-track swathes of data about six times the value of the water depth along tracks. The Simrad EM300-Dual system, operated aboard the RV 'le Suroit', allows recording swath data only with a track-spacing of about twice the water depth. Although the two data sets have different resolutions (a 100/150-m precision for EM-12 data and a 30-m precision for EM-300 data), they were merged and processed as a unique grid (with a pixel size of 50 m) using Ifremer's Caraïbes software package. During both surveys, deeper subbottom structures, at penetration sometimes up to 3 s TWTT (two-way travel time; about 3 km), were also imaged using a 75-cubic-in. Soderia GI gun and a six-channel streamer. We, therefore, obtained a total of about 5000 km of continuous geophysical data over most of the NDSF (see track lines on Fig. 1). In 2002, the 'Medisis' survey, run onboard the R.V 'Le Nadir', provided an additional grid of 1500 km of deep-penetrating, multichannel seismic (MCS) data (360 channels) (Fig. 1). These new data have yielded seismic data reaching locally down to 11 s TWTT (around 20/22 km). On these data salt structures and deeper, subsalt structures along the Egyptian margin are particularly well imaged (Masclé et al., 2003). In some key areas, our data set has been complemented by sections and coherency maps from seismic-reflection data provided by BP-Egypt.

In order to better assess the impact of salt tectonics on 3D geometry of the NDSF, we conducted coeval analyses of available bathymetric and seismic data to construct tentative isopach maps of the (1) Messinian mobile layer (i.e. the seismically transparent salt layers) and (2) its brittle sedimentary overburden (i.e. the upper evaporites/Messinian clastics and Plio-Quaternary deposits). In constructing these maps, we assumed a value for the mean seismic velocity of 2 km/s for the brittle sediment overburden and a value of 4 km/s for the salt layer (Schreiber et al., 1973; Ross and Uchupi, 1977). These maps have a vertical resolution on the order of 200 m for the lower evaporites (0.1 s TWTT) and 100 m (0.1 s TWTT) for the sedimentary overburden. Because of the seismic grid size, their lateral resolution is about 10 km. Finally, we calculated the depth of the Messinian unconformity or base of salt with respect to the present-day sea floor by simply subtracting data from the two isopach maps from bathymetric data.

Before discussing these maps, we must warn readers that the base of the Messinian salt layer is locally hard to image because of restricted seismic penetration and interferences with the first sea-bottom multiple, thus obscuring the base salt. Consequently, isopachs of the salt layer are not as accurate as isopachs of the overburden. The resulting map of the Messinian surface depth must, therefore, be interpreted with care. Moreover, Ross and Uchupi (1977) pointed out that seismic velocities within the evaporites can vary according to the percentage of high-velocity halite and low-velocity clastics. Not accounting for these effects, as we did not, can introduce significant errors to estimating evaporite thickness.

4. Results

4.1. Structural analysis of the NDSF

4.1.1. Impact of evaporite distribution on sedimentary overburden deformation

Near the shelf, Messinian clastic deposits are commonly interfingered with coeval evaporites, affecting the overall rheological behavior of the Messinian sediments and making them less mobile. Therefore, delineating lateral changes in facies of the Messinian series is a fundamental key in understanding how the Plio-Quaternary NDSF was affected by salt tectonics. Knowing the lateral extent of the mobile evaporites and the less mobile Abu-Madi Formation allows us to distinguish different rheological domains within the deep-sea fan: (1) a lower-slope evaporitic, halite-rich, and mobile domain; (2) a middle-slope domain, where evaporites and clastics are interfingered and thus less mobile (somewhat similar to a Messinian detrital cone); and (3) a domain totally devoid of Messinian evaporites (Fig. 4). This last domain can be correlated either with the pre-Messinian platform deeply incised by numerous canyons (Messinian badlands)—and probably with the upper part of the Messinian detrital cone or with topographic highs that emerged during the Messinian sea-level fall (e.g. ESM). Both represent stable domains that have not been affected by salt tectonics.

In our study area, the southern boundary of the mobile salt layer corresponds in most cases to the edge of the pre-Messinian incised continental shelf (Aal et al., 2001) located downslope from the present-day continental platform (Fig. 4) and sometimes with a smoother surface, probably corresponding to a Messinian detrital cone. The edge of the inherited pre-Messinian shelf is characterized, especially in its eastern part, by a steep cliff or scarp, on the foot of which normal growth faults nucleated. This inherited pre-Messinian shelf forms a promontory centered around 30.30° E longitude (Fig. 4). Its shape appears to be controlled by two subsalt fault systems that are now more or less inactive. Its western edge is bounded by a main NE-SW fault zone thought to be a reactivated Jurassic lineament (Aal et al., 2000), whereas its eastern corner is shaped by a N-S fault that may be interpreted as the aborted, northward prolongation of the Suez rift system (Masclé et al., 2000). Above this Messinian 'promontory', the Plio-Quaternary sediments are nearly horizontal and show little or no deformation because there were virtually no mobile Messinian evaporites deposited in this area (see stable shelf in Fig. 4). The boundary between the mobile and non-mobile domains is consequently very clear on both seismic-reflection data and on the present-day bathymetric maps: the upslope, poorly deformed area can be distinguished easily from the downslope domain where the Plio-Quaternary cover is often strongly deformed by gravity-driven salt tectonics. In the western part of the fan, the Messinian canyons are particularly abundant, and the transitional area, characterized by the interfingering of the Abu-Madi formation and the evaporites is wider. Consequently, the boundary between mobile and non-mobile domains is located farther downslope in this area (Fig. 4). Such

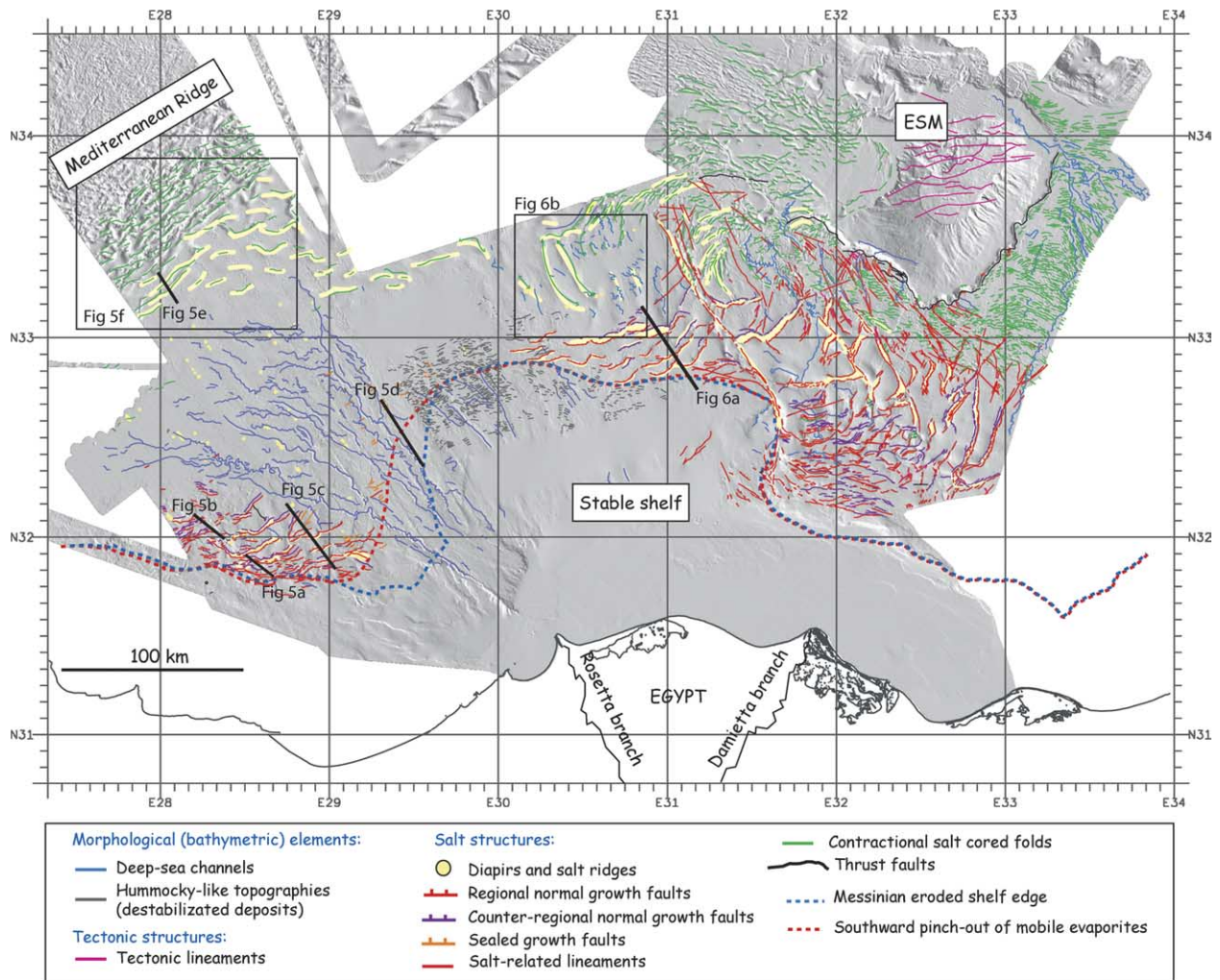


Fig. 4. Morphostructural map of the NDSF (see legend). Blue dotted line = limit of Messinian eroded shelf domain. Red dotted line = southern edge of Messinian salt extension. Area north of red line = mobile rheological domain. South of red line = non-mobile rheological domain. Areas between red and blue lines = areas where both detrital (Abu-Madi) and evaporitic sediments are observed (for interpretation of the references to colour in this figure legend, the reader is referred to the web version of this article).

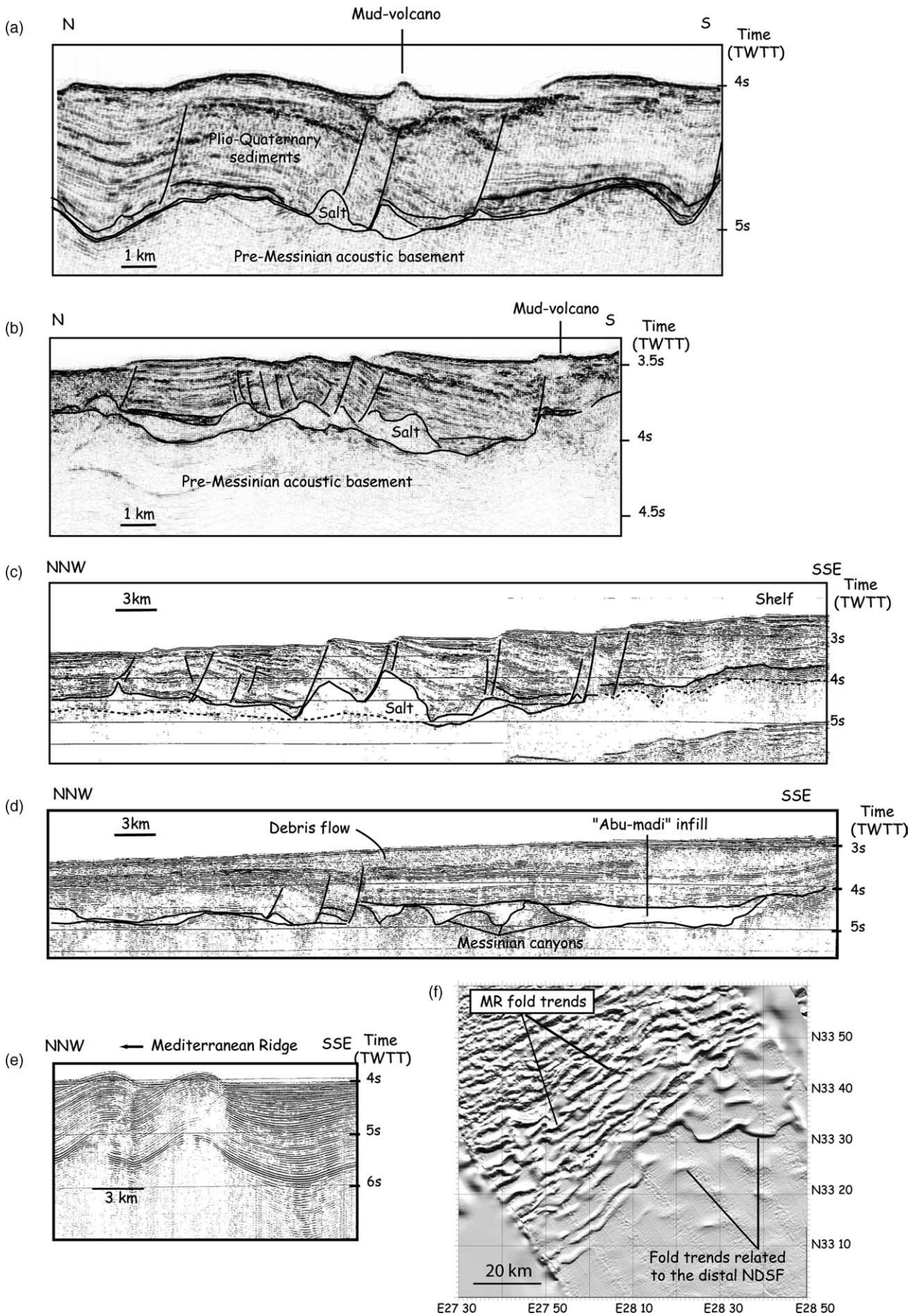
facies variations, as well as the presence of Messinian paleohighs have direct bearing on subsequent gravity tectonics. Areas that were exposed during Messinian times, such as ESM, constitute now 'solid or rigid cores' in the middle of a region underlain mostly by mobile Messinian evaporites. Two main Messinian paleohighs exist in the NDSF area and have acted as stable areas during Plio-Quaternary tectonics. The first one is the incised continental platform and its associated clastic cone; the second one is Eratosthenes Seamount.

4.1.2. Deformation patterns within the salt-bearing basin

Because salt tectonics in the NSDF is currently active, salt structures (growth faults, folds, salt ridges, and massifs) deform the present-day seafloor and can be identified on bathymetric maps. By combining the interpretation of both 2D seismic profiles and surface bathymetric data, we are able to determine the 3D geometry of salt structures with a reasonable degree of confidence. According to our data, seafloor morphology in the salt-bearing part of the deep-sea fan, shows strong variations. If bathymetric and backscatter data are

examined, three morphostructural provinces are visible—the Western, Central, and Eastern provinces (Figs. 1 and 4) (Bellaiche et al., 1999, 2001; Gaullier et al., 2000; Mascle et al., 2001; Loncke et al., 2002a).

4.1.2.1. Western province. Bounded on the north by the Mediterranean Ridge accretionary complex, the western province is characterized mainly by a well-developed channel-levee system, proximal normal growth faults, and distal contractional folds (Fig. 4). Within the upslope part of this province, the structural style of the overburden varies with the initial thickness of the mobile evaporitic layer. In the west, where the base salt is higher and, hence, the salt layer initially thinner, overburden extension was accommodated by both regional and counter-regional normal growth faults. These growth faults have arcuate traces and form a belt that closely parallels the southward (i.e. updip) salt pinch-out. Some are associated in sets to form wide grabens underlain by salt (Fig. 5b). Also common in this area are turtle-structure anticlines overlying salt welds. There,



the mobile salt has been withdrawn entirely, forcing overlying sediments to bend and mimic the shape of the underlying Messinian subsalt strata (Fig. 5(a) and (b)). Because eastward, the salt base deepens, the salt must have been initially thicker. Turtle anticlines are progressively replaced by regional and counterregional normal growth faults (\sim E28–29°), then by regional normal growth faults only (\sim E29°) (Fig. 5(c)). Finally, in the easternmost area (\sim E29°.15–30), the growth fault system is no longer visible on bathymetric data (Fig. 5(d)). On seismic-reflection data, however, growth faults are still visible, but they are sealed by thick (500 m thick on average) debris-flow deposits.

The midslope area (\sim N32.10–33°) commonly comprises salt ridges and diapirs (Fig. 4). The salt layer thickens (up to 3 km) at the base of the slope and near the Mediterranean Ridge. Present-day northward salt thickening results from (1) an initially greater salt thickness at time of deposition (greater bathymetric depth during Messinian times) and (2) genuine tectonic thickening of seaward downslope translation of the overburden located on the middle and upper slopes, which generate horizontal shortening near the base of the slope, effectively ‘bulldozing’ and thickening the salt layer. Contractive tectonics in the distal part of the NSDF (\sim N33.10°) is marked by a train of E–W-trending salt-cored buckle anticlines (Fig. 5(e) and (f)). We interpret them as reflecting the distal contraction associated with gravity gliding/spreading of Messinian evaporites and their overburden. These folds differ from the NE–SW-trending ones that characterize the Mediterranean Ridge toe (Fig. 8(f)).

4.1.2.2. Central province. The central province displays similar morphostructural characteristics, except that channels have been erased and/or dislocated by recent debris flows and are thus far less abundant (Fig. 4). Within this province, the southward salt pinch-out matches the limit of the pre-Messinian shelf that forms a promontory extending up to N32.40. North of this promontory, sedimentary overburden thicknesses are up to 2.5 km, whereas evaporites are very thin. A 200-km-long growth-fault belt, well expressed on bathymetric data, lies east of the promontory. Little salt remains, except for a few salt rollers located beneath the growth-fault footwalls (Fig. 6(a)). There again there is a strong contrast between the little- or undeformed post-Messinian shelf sediments and sediments in the salt basin deformed by growth faults and rollover anticlines (Figs. 4 and 6(a)). Midslope, NW–SE, N–S, and E–W-trending salt-cored folds are present (Fig. 6(b)). The resolution of our seismic-reflection data did not allow us to correlate these folds with subsalt structures in the pre-Messinian series. The three fold families interfere to form polygonal or subcircular minibasins clearly visible on bathymetric data (Fig. 6(b)). Lateral changes in salt and overburden thickness can be

matched to bathymetric features: elongate and arcuate bathymetric highs are underlain by salt pillows, whereas bathymetric lows correspond to thick synformal sediment depocenters.

Distally the brittle overburden thins progressively, whereas the salt thickens. The distal edge of the central province is, however, not fully imaged on our data set. Assuming that it is similar to that of the western province, the distal part would be in contact with the southern edge of the Mediterranean Ridge.

4.1.2.3. Eastern province (including the Levant). The eastern NDSF province differs markedly from the western and central provinces. It comprises a NNW–SSE-trending tectonic corridor that is clearly visible on the bathymetric map (Figs. 4 and 7) and contains numerous salt structures (>250 km long, 100 km wide). Unlike in the other two provinces, the main structural trends are oblique with respect to the local bathymetric slope. The presence of this oblique tectonic corridor introduces a significant asymmetry in the overall physiography of the NDSF. This asymmetry is accentuated further by the presence of the Eratosthenes Seamount in the north of the province.

Seafloor deformation. Bathymetric data from the eastern and Levantine provinces (east of ESM) show seafloor deformation patterns consistent with thin-skinned gravity tectonics above salt, including extensional structures upslope (crestral grabens, growth faults) and contractional structures downslope (Figs. 4, 7 and 8). A 400-m-high, semicircular scarp wraps around the base of the Eratosthenes Seamount (except along its northern slope). The scarp is similar to the Sigsbee Scarp in the US Gulf of Mexico (Diegel et al., 1995) and corresponds to the distal edge of the Nile cone and the seaward salt pinch-out in this province (Figs. 4 and 7).

Detailed structural analysis of the tectonic corridor emphasizes the following characteristics (Figs. 7 and 8):

- (1) The corridor consists of a series of sublinear, NNW–SSE-trending fault zones and associated salt structures that bound overburden blocks ranging from 10 to 50 km in width. Within these blocks, channel systems are either guided or disrupted by movement along the fault zones, suggesting that the faults have been recently active (Loncke et al., 2002a).
- (2) The NNW–SSE-trending faults are undergoing strike-slip movement (Fig. 7). The fault set forming the west boundary of the corridor is experiencing left-lateral slip, as interpreted from en echelon fold patterns, whereas the east-bounding fault zone has right-lateral slip, recorded by en echelon sigmoidal crestral grabens having a planform geometry similar to that of tension gashes (Fig. 7). Overall,

Fig. 5. Seismic lines characterizing the western province (see location on Fig. 4). In the extensional domain, from west to east: (a) normal growth faults rooted on Messinian salt. (b) Turtle anticline structure. (c) Faulted Plio-Quaternary depocenters. (d) Sealed growth faults and buried debris flows. In the contractional domain: (e) Distal salt-cored folds. (f) Bathymetric zoom on angular unconformity existing between E–W gravity-driven contractional folds and WSW–ENE folds characterizing accretionary Mediterranean Ridge trends.

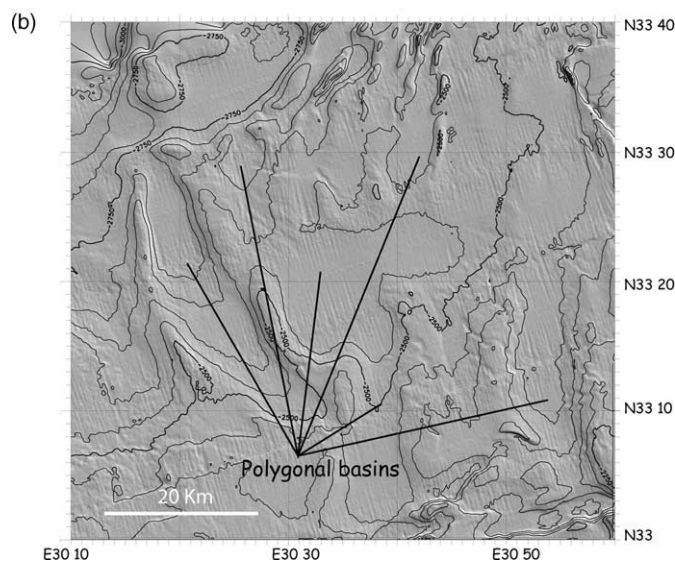
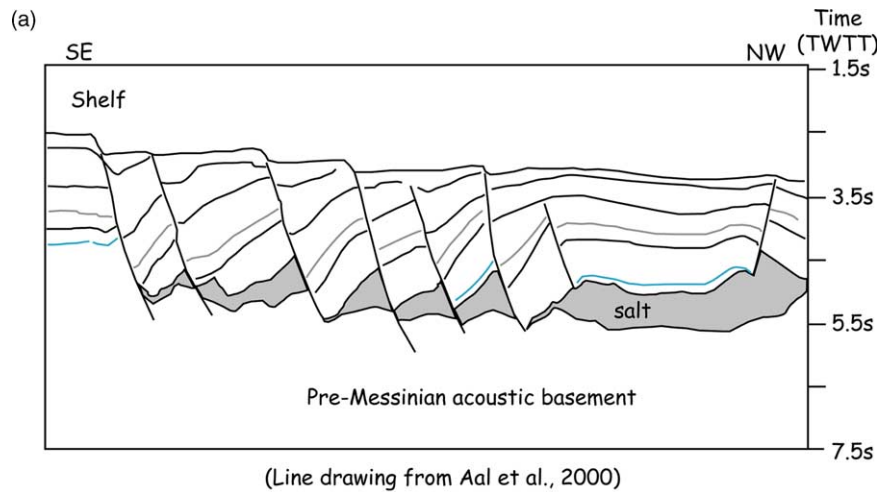


Fig. 6. (a) Line drawing of seismic line characterizing upper central province (see location on Fig. 4). (b) Bathymetric detail of downslope minibasins (see text for details).

the movement along the NNW–SSE fault system is transpressional in the northwest area and transtensional in the southeast area.

- (3) In the east, the NW–SE-bounding faults are replaced progressively by an echelon grabens (Fig. 7).
- (4) In addition to this structural pattern, there are also features typical of gravity spreading above salt. These include proximal regional and counter-regional normal growth faults, midslope polygonal minibasins bounded by salt ridges, and distal buckle folds (Fig. 8(a)).
- (5) Structural analysis allows us to estimate the direction and sense of recent movements of the salt and its overburden. Within the corridor itself, the sediment overburden has spread toward the NW, as recorded by the widening of E–W and SW–NE grabens and the strike–slip along NNW–SSE faults. In contrast, in the east part of the corridor, sigmoidal crestal grabens and contractional folds indicate that spreading took place toward the north and the east (Fig. 7).

Deep, subsalt structural pattern. Seismic-reflection data reveal that the NNW–SSE fault trends in the overburden are often associated with deep, narrow, salt ridges (Fig. 8(b)). To the north, these salt ridges are pinched off, which suggests that the ridges were first emplaced in a thin-skinned extensional regime and later reactivated in a transpressive regime (Fig. 8(c)).

Within the corridor itself, the structural pattern is consistent with overall downslope gravity spreading:

- (1) The upslope part of the corridor comprises many closely spaced normal faults verging either updip or downdip. These faults result from the collapse of bowl-shaped depocenters that were initially bounded by growth faults and salt ridges and then unfolded and became anchored onto the pre-Messinian basement once the salt layer became very thin (Figs. 7 and 8(a)). There, the brittle overburden is particularly thick, and the only salt structures are relict salt rollers, associated with growth faults bounding the collapsed depocenters.

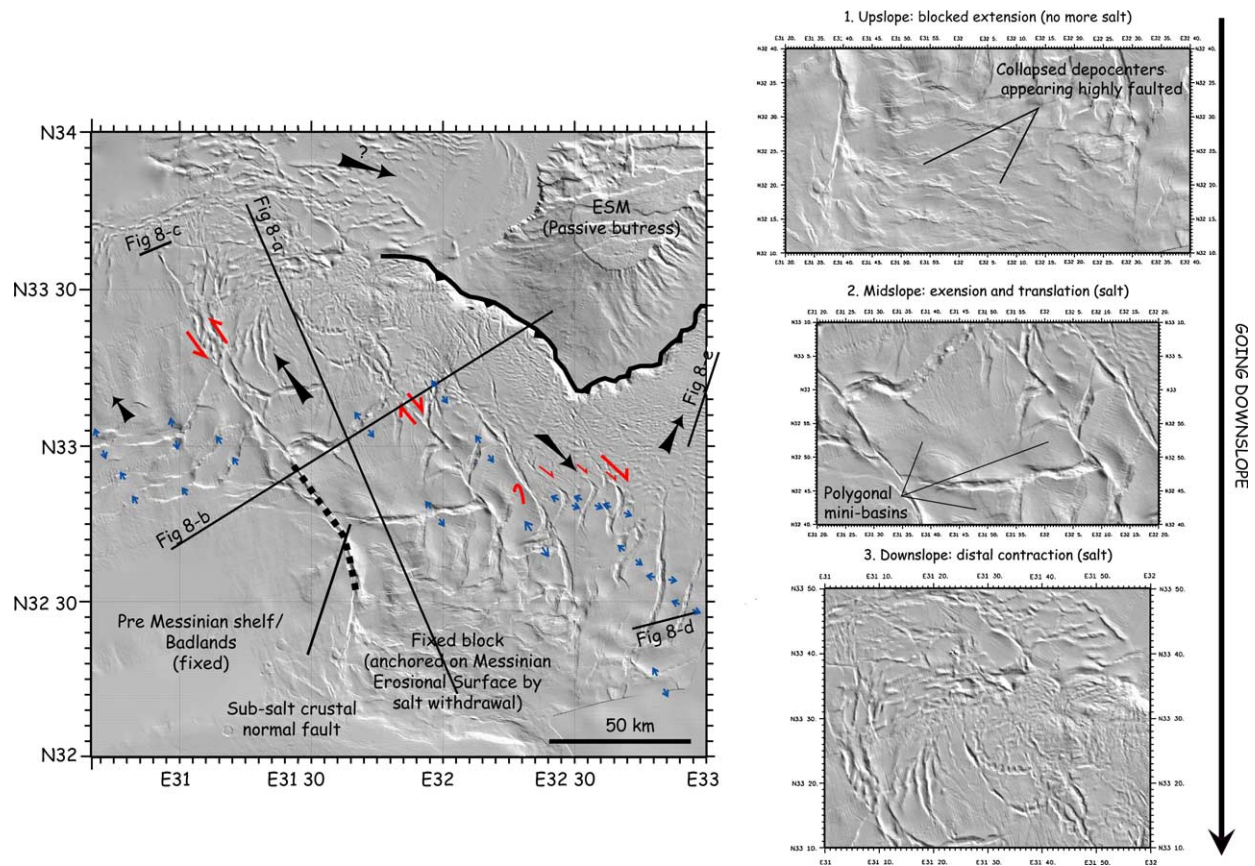


Fig. 7. Shaded bathymetry of eastern province with kinematic interpretation.

- (2) In the midslope area, a network of polygonal sediment depocenters are bounded by E–W and NW–SE normal faults and grabens underlain by reactive salt ridges (Figs. 7 and 8(a) and (b)). The mobile salt layer is thicker (up to 200 m), whereas the Plio-Quaternary thickness is similar to that upslope. This system can be interpreted as an extensional salt system that is less ‘mature’ than the one upslope.
- (3) In the distal area, toward the abyssal plain, normal faults progressively disappear, whereas arcuate contractional salt ridges, closely spaced folds and thrusts dominate (Fig. 7(a)–(c)). The overburden thickness decreases, whereas the salt layer thickens up to 3 km. To the northeast, spreading is blocked by the Eratosthenes Seamount, which acts as a distal buttress.

East of the tectonic corridor, in the Levantine province of the deep-sea fan, the contractional domain is characterized by arcuate, closely spaced folds, and its distal edge is marked by a bathymetric scarp surrounding the ESM (Figs. 4 and 8(b) and (e)). The short fold wavelength is related to the low thickness of underlying evaporites: whereas the mobile Messinian evaporitic layer is 1 km thick south of the ESM, it is merely 200 m thick east of the seamount (Fig. 8(e)). South and west of the seamount, loading of the salt layer and seaward gravity spreading of the prograding sediments contributed to inflating of the distal salt layer, which encroaches onto the base of the

seamount. Therefore, the present-day limit of this partly allochthonous salt mass lies higher and farther north than the initial, depositional limit of the autochthonous salt (Gauquier et al., 2000). Near the bathymetric scarp, the salt is often stacked up in nappes and overthrust, causing local thickening of the salt layer (up to 1400 m). The fold direction indicates that the sedimentary overburden spread northward, in the south and east of the ESM. This spreading direction controls the geometry of the thrusting contacts between the stable seamount and the mobile salt and sedimentary overburden, causing the bathymetric scarp surrounding the southern ESM domain to have a subcircular trace (Figs. 4 and 7).

Finally, the southeast transtensional limit of the tectonic corridor contains several sigmoidal grabens (Fig. 8(d)) that change along strike into narrow lineaments, which correlate on seismic data with negative flower structures. The latter features are much younger than grabens in the corridor.

At this stage, our structural analysis suggests that the tectonic corridor may owe its origin to three features:

- Northwestward gravity spreading and associated strike–slip movements may be caused by the presence of a subsalt, fault-controlled graben that ‘channelled’ spreading direction.
- The Eratosthenes Seamount, acting as a distal buttress, may have blocked northeastward gravity spreading, thereby reorienting the direction of gravity spreading toward

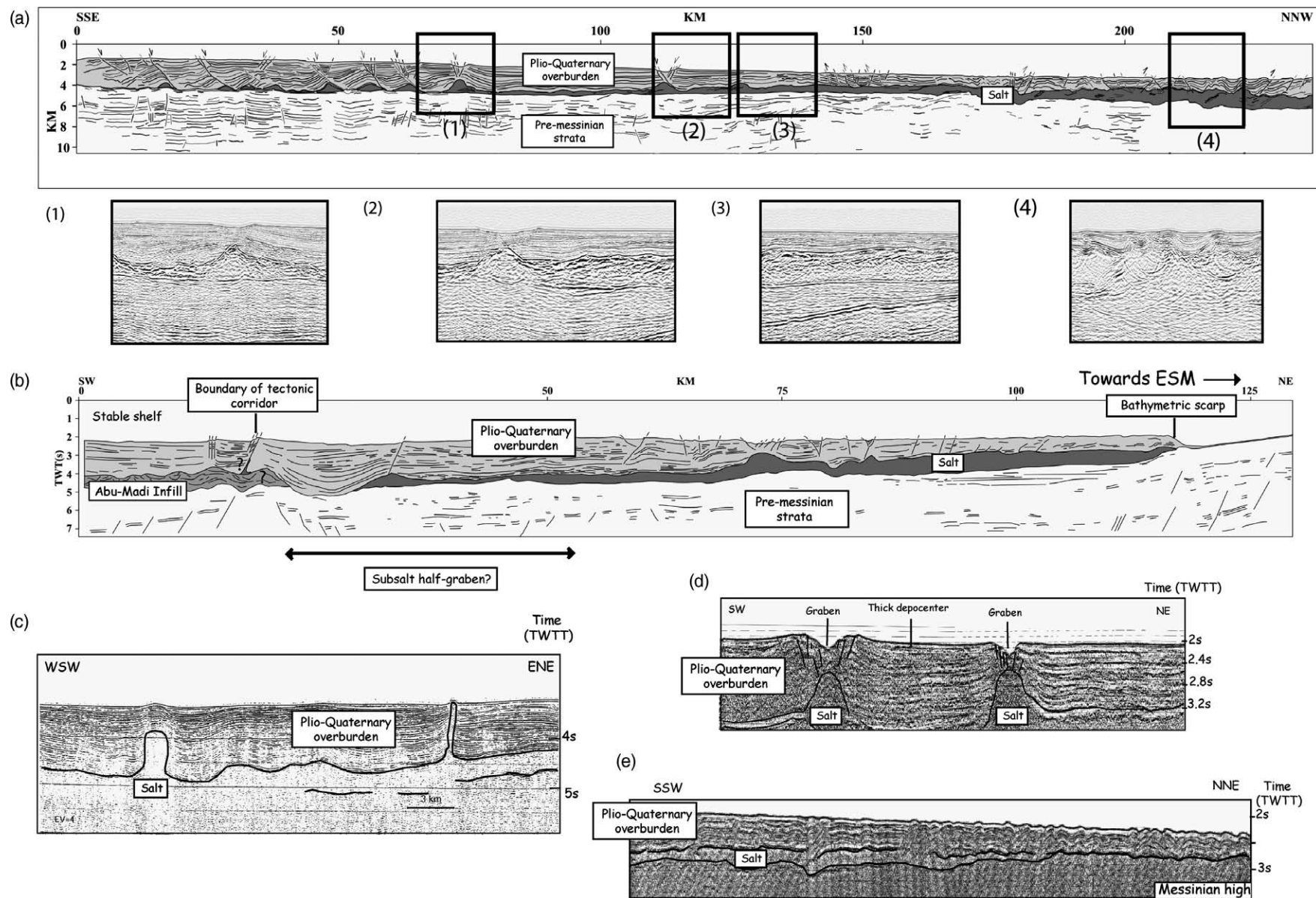


Fig. 8. Deep structure of eastern province. (a) Deep, penetrating, seismic line crossing NNW–SSE tectonic corridor. (b) Line drawing of a deep, penetrating, seismic line crossing transversely the NNW–SSE tectonic corridor. (c) Seismic line crossing distal pinched diapirs. (d) Typical crestal grabens observed in easternmost part of this province. (e) Eastern deep extension of the Eratosthenes Seamount.

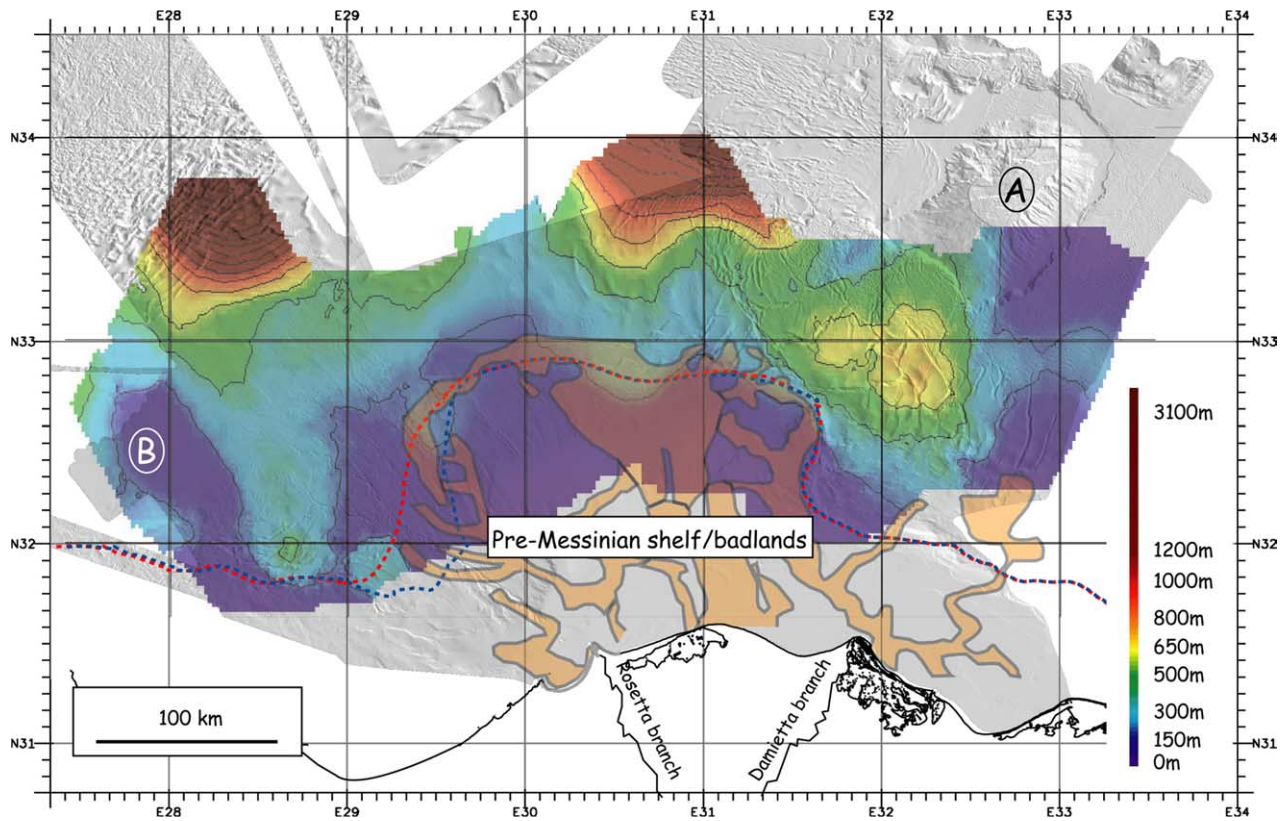


Fig. 9. Isopach map (in meters) of lower mobile evaporites overlain on shaded bathymetry of NDSF. Messinian canyons represented in orange (defined by Abdel Aal et al. (2000) and completed by our data set). Areas A and B are two Messinian bathymetric or topographic highs onto which no salt was deposited (for interpretation of the references to colour in this figure legend, the reader is referred to the web version of this article).

the NW and SE. This scenario would also explain the transpressional regimes near the ESM.

- The N–S to NW–SE corridor may be caused by the shape of the landward salt pinch-out, itself controlled by subsalt basement faults bounding the east side of the shelf promontory and trending N–S to NW–SE.

4.2. Influence of Messinian topography on thin-skinned tectonics

4.2.1. 3D geometry of mobile Messinian evaporites and brittle overburden

On isopach maps of both mobile evaporites and Plio-Quaternary sediments (Figs. 9 and 10), the overall sediment distribution is radial, suggesting that the dominant deformation process is gravity spreading. The brittle Plio-Quaternary sedimentary overburden is thinning radially downslope, whereas the mobile evaporitic layer thickens radially. This pattern results from the radial downslope flow of the salt in response to sedimentary loading in the proximal part of the margin. Indeed, the two isopach maps (salt and overburden) are ‘inverted images’ of one another: the thickness of Plio-Quaternary overburden reaches up to 3 km in the proximal area, where salt is thin, whereas the Messinian salt is as thick as 3 km near the base of the slope, where the sediment overburden is thin. The overall trends that can be extracted from analysing

the isopach maps are two: (1) the Plio-Quaternary overburden is particularly thick (2.5 km on average) above the pre-Messinian continental shelf. This thickness may be related to the wide extent of the shelf, whose width can reach locally up to 150 km. Such a wide shelf would have trapped a large part of the sediment supply. (2) The evaporitic layer may have moved seaward as it was loaded under Plio-Quaternary sediments upslope, and the south limit of thick salt has migrated northward through time (blue areas in Fig. 9).

Isopach maps also indicate the presence of two specific pre-Messinian, paleo-bathymetric features (A and B in Figs. 9 and 10) that have affected the patterns of thin-skinned tectonics and may explain the structural asymmetry of the deep-sea fan:

- The first paleo-bathymetric feature is the Eratosthenes Seamount (A in Figs. 9 and 10). The bathymetric scarp located at its base clearly marks the distal edge of the Messinian salt. East of the ESM, the salt layer is very thin. This bathymetric high behaves as a fixed and rigid core in the middle of a region where the overburden above the salt is mobile. The presence of such a fixed core may have (1) partly blocked northeastward gravity spreading, (2) generated some component of transpressional strain along the NW–SE-trending fault zones, and (3) led to the formation of distal arcuate folds wrapping around the seamount.
- The second paleo-bathymetric feature is located in the westernmost region of the deep-sea fan (B in Figs. 9 and 10).

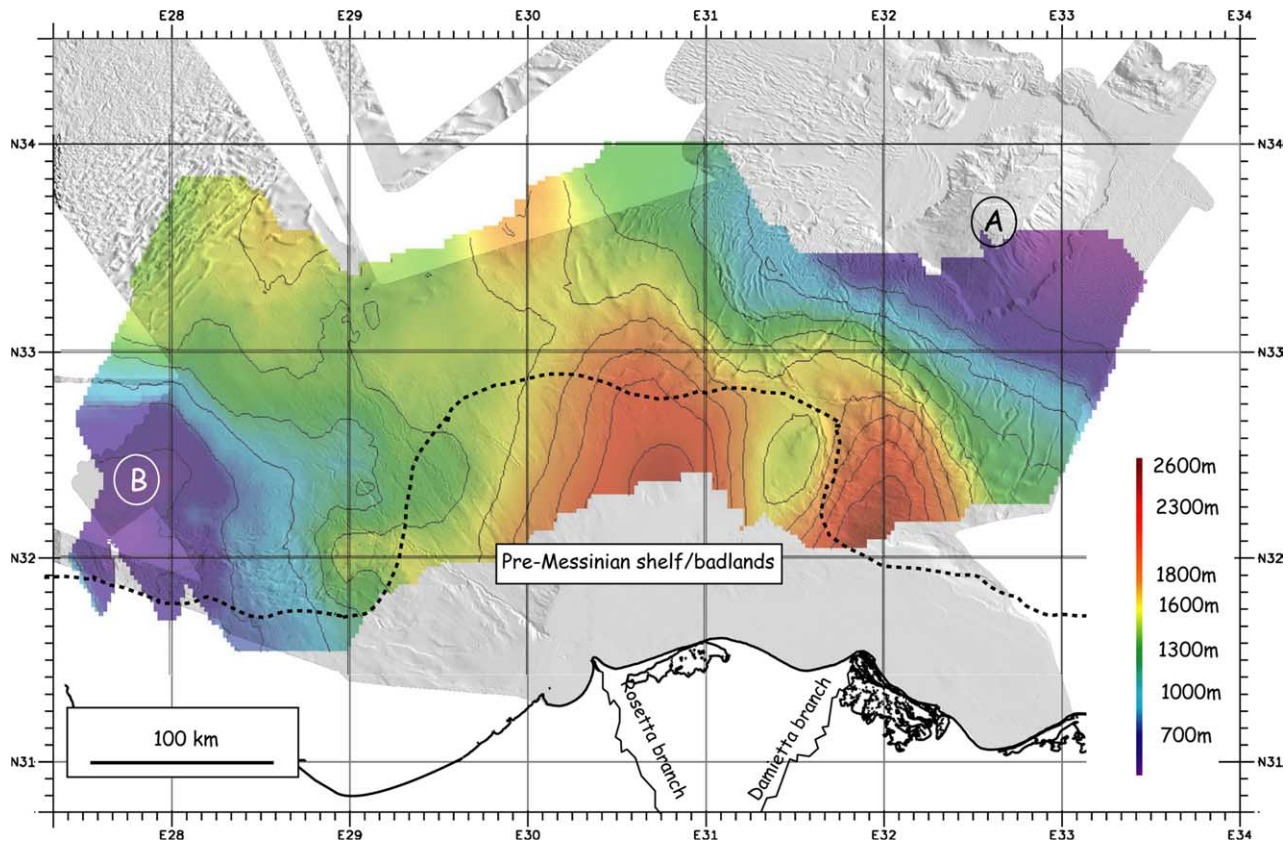


Fig. 10. Isopach map (in ms) of brittle sediments (detritic Messinian layers + Plio-Quaternary overburden). A and B = two Messinian relief devoid of Messinian salt.

During Messinian and Plio-Quaternary times, the sedimentation rates in the western province of the NDSF were lower than those in the other two provinces. There is even evidence that no salt was ever deposited in an area located about 100 km from the southern salt pinch-out (B in Figs. 9 and 10). According to our mapping, this area correlates with a pre-Messinian high (~ 30 km wide and 50 km long) where the salt thickness was greatly reduced. In contrast with the adjacent areas, where the cover is deformed, the Plio-Quaternary cover resting on this paleo-high is largely undeformed.

Finally, in the eastern tectonic corridor, no clear subsalt graben is obvious beneath the NW-SE structures. However, in the southern part of the corridor, Plio-Quaternary thicknesses are larger than in the adjacent, pre-Messinian platform area, suggesting that there is some sort of pre-Messinian half-graben.

4.2.2. Gravity spreading versus gravity gliding

Ryan (1978) published a preliminary isochron map in TWTT (two-way travel time) of (1) the Messinian unconformity and (2) the base salt (both of which he gathered as one surface) in the eastern Mediterranean. His map shows two subbasins separated by the Eratosthenes Seamount: the shallow Byblos basin to the east and the deeper Xenophon basin to the west. As informative as it is, this isochron map must be interpreted with caution because it does not account for the

faster seismic velocities within the thick basinal evaporites. In our own analysis, we used different seismic velocities for the evaporitic layers and the Plio-Quaternary sediments in order to map the Messinian unconformity and base of salt more accurately. Although uncorrected for thermal subsidence and isostatic variations, the present-day base of the Messinian salt, i.e. the pre-Messinian morphology, as deduced from the combined brittle and mobile isopach maps (Fig. 11) provides some interesting insights. In particular, it shows the existence of pre-Messinian bathymetric highs. One of these highs corresponds to the Egyptian margin eastern province where the ESM clearly extends southeastward, although now being covered by thin Plio-Pleistocene sediments. The ESM separates two basins, as already indicated by Ryan (1978). Using the depth of the unconformity we can estimate the respective slope gradient of the two basins. The western and deeper Xenophon basin (corresponding to our western and central provinces) has a seaward slope gradient averaging 1° , whereas to the east, the Byblos basin (corresponding to our eastern and Levant provinces) shows a 0.6° dipping slope to the south. Such difference in slope gradients for the base of the evaporites suggests that the two basins deformed by different gravity processes (spreading or gliding), which may explain the differences in salt-tectonics style within the NDSF. For example, the trend of salt structures in the western and central provinces is perpendicular to the slope, an orientation that is consistent with a seaward gravity-gliding process. In contrast,

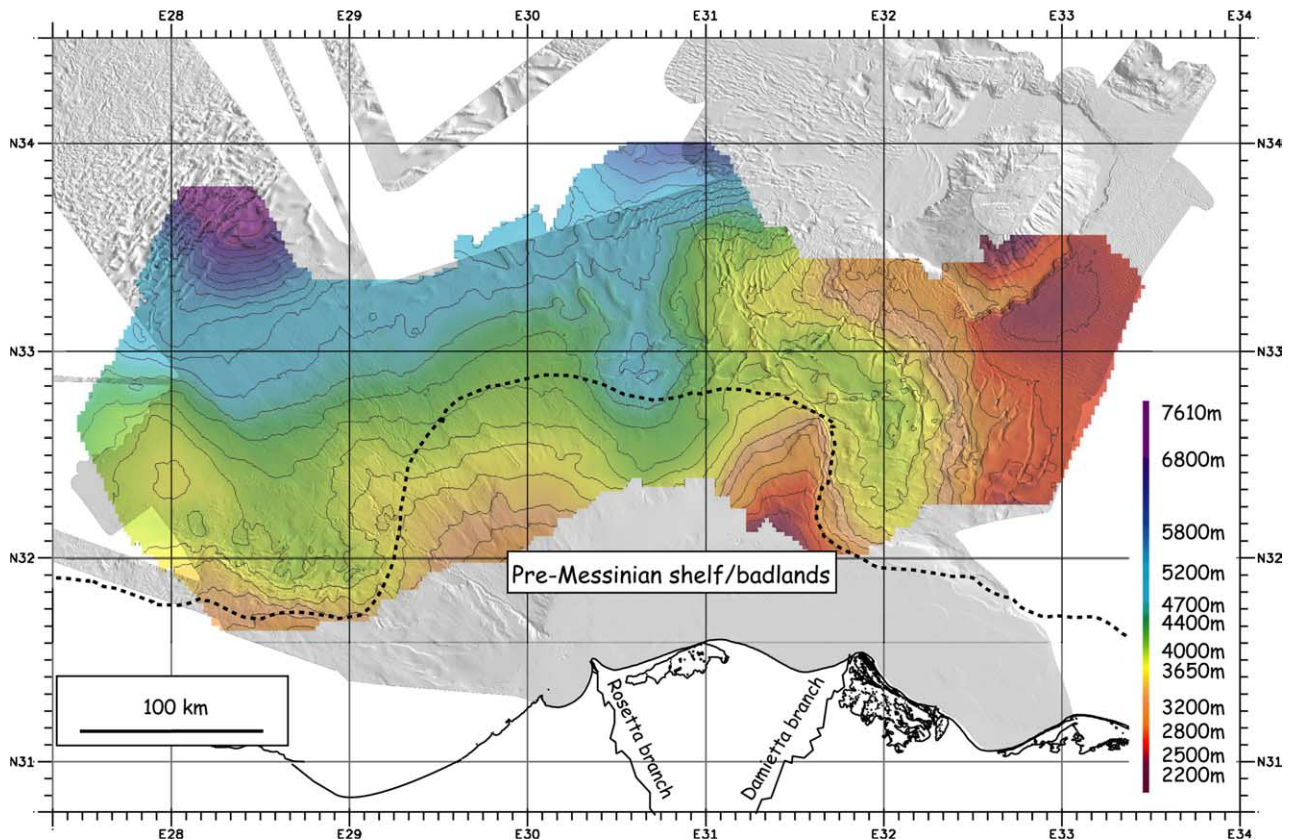


Fig. 11. Present-day base of salt (basinward) and Messinian erosional surface (landward), as deduced from present-day bathymetry, mobile and brittle isopachs.

the trends of salt structures in the eastern and Levantine provinces are multidirectional (e.g. faults bounding the minibasins), which is more consistent with deformation by gravity spreading (Rowan et al., 1999).

It is interesting to notice also the presence of a deeper channel within the central province, under the well-expressed growth faults illustrated on Fig. 6. A greater salt thicknesses may account for the vigorous extensional activity recorded in this area.

5. Synthesis and discussion

Our results concerning the shallow structure of the NDSF can be synthesized as follows:

In all four morphostructural provinces the structural pattern observed on dip-oriented seismic lines is typical of salt-bearing passive margins undergoing gravity spreading and/or gliding. This pattern includes proximal extensional and distal contractional structures. The isopach map of the Pliocene-Quaternary and clastic Messinian sediments (Figs. 9 and 10) emphasizes just such a homogeneity throughout the deep-sea fan: the overburden distribution is radial, with two main depocenters, one located in the central province, the other in the southern part of the eastern province. As the brittle sedimentary overburden thins progressively downslope, the thickness of the mobile Messinian salt increases. This pattern results from two processes. First, proximal sedimentary loading has induced

some amount of seaward salt migration and distal inflation. Second, as the thick depocenters were translated seaward, the salt layer and its thin overburden located downslope from the depocenter were pushed forward, bulldozed, and thickened. Brittle sediment thickness can reach nearly 2.5 km, whereas salt thickness reaches up to 3 km toward the abyssal plain and 1 km toward the ESM.

At first glance, the deformational pattern and the overall radial sedimentary distribution of the Plio-Quaternary NDSF appears to be that of a lobate sediment package of regional scale that merely spread radially under the effect of gravity. However, more detailed analysis reveals that the deep-sea fan is strongly asymmetric, especially when one compares the eastern and western provinces in terms of fault patterns in the Plio-Quaternary section: in the west, normal growth faults in the upslope region trend about parallel to the coastline, and the overburden in the midslope domain merely underwent translation with little or no deformation. In contrast, in the east, the entire overburden wedge deformed, and thin-skinned extension was accommodated by two orthogonal sets of normal faults arranged in a NNW–SSE tectonic corridor.

Several geological characteristics of each of the eastern and western provinces may explain why their structural styles differ. These are differences in (1) the subsalt tectonic architecture, including active or dormant basement faults; (2) the dip and 3D geometry of the base salt; (3) the estimated salt thickness when thin-skinned salt tectonics began; and (4) the

presence (and location with respect to the overall deep-sea fan) of areas entirely devoid of mobile salt that acted as ‘anchor points’ during Plio-Quaternary times.

The first hypothesis presented by Mascle et al. (2000) involves the possible influence of an active NNW–SSE-trending graben in the subsalt basement. This graben would represent the northern extension of the Rift of Suez and would have propagated upward through the salt, thus creating the NNW–SSE tectonic corridor within the overburden. This hypothesis, however, is opposed by the following observations: unlike what bathymetric data suggest with the presence of linear continuous NW–SE faults, seismic-reflection data (cross-section (b) in Fig. 8) does not show any significant basement control in the area near the Eratosthenes Seamount (NE in cross section (b), Fig. 8). Instead, the section shows a gradual deepening of the base salt toward the SW. Landward the section shows an abrupt rise of the base of the overburden at the paleo-Messinian shelf break (SW part of profile (b) in Fig. 8). On one hand, this rise or scarp could be interpreted as an offset

resulting from slip along a basement step; in this case, the basement structure underlying the NNW–SSE tectonic corridor would be a half graben bounded by a single basement fault whose location coincides with the scarp of the paleo-Messinian shelf break (Aal et al., 2000). On the other hand, this offset may not have a structural origin and could merely represent the transition between the clastic Messinian rocks and the Messinian evaporites.

In any case, the surficial fault marking the western boundary of the corridor extends well beyond (to the NNW) the area where the basement fault is present. Therefore, the western limit of the corridor is a thin-skinned tectonics fault rather than a deep-seated crustal structure.

Instead, we favor the hypothesis that the thin-skinned Plio-Quaternary structural pattern is related to the Messinian paleo morphology of the Nile deep-sea fan, which controlled both the thickness of the mobile salt layer and the slope of the base salt. Both the structural analysis and isopach maps suggest that the asymmetry of the deep-sea fan is related to the presence, below the Plio-Quaternary

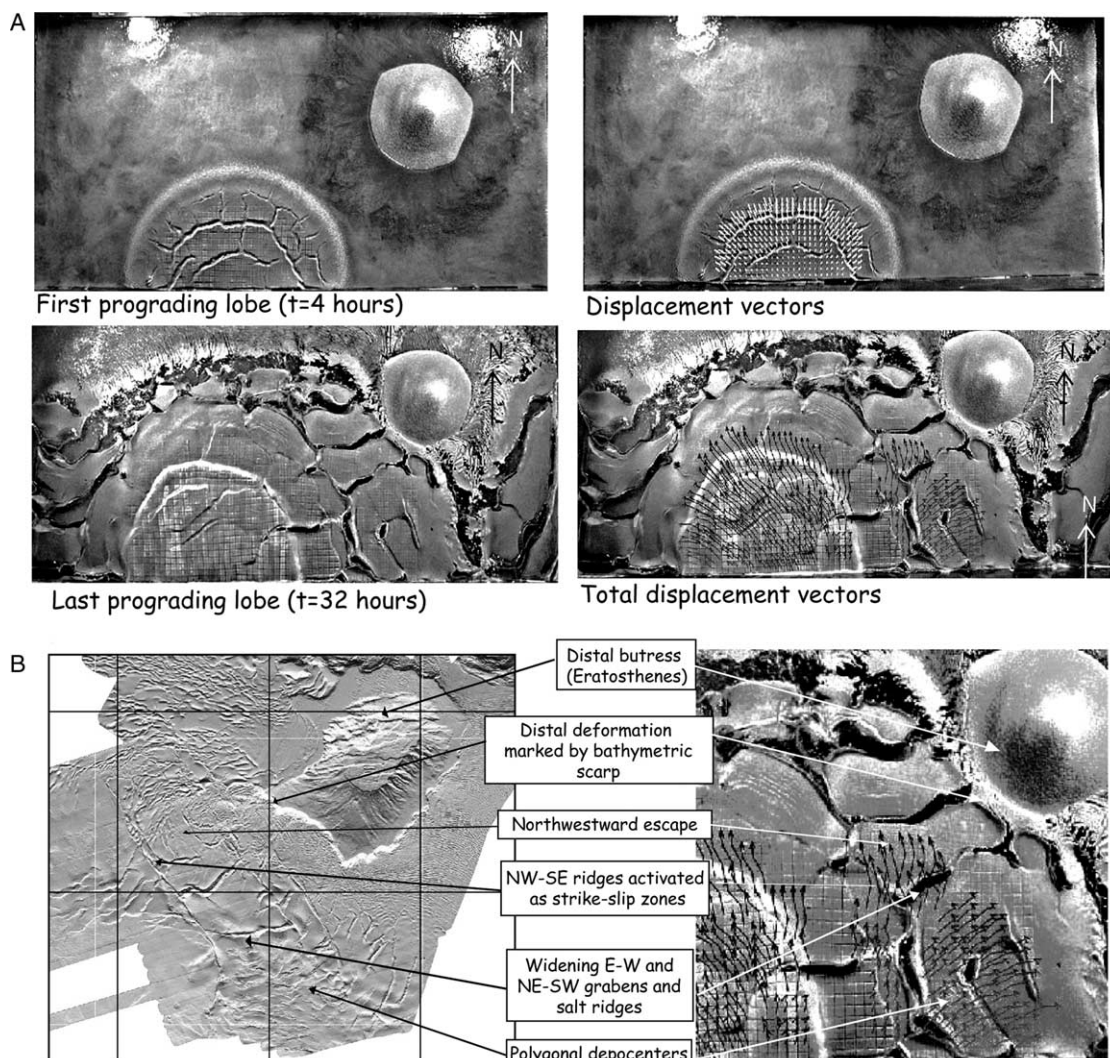


Fig. 12. (A) Experiment testing the effect of a passive buttress on the gravity spreading of a sedimentary lobe. (B) Comparison between final deformation pattern of the experiment and the eastern NDSF.

cover, of pre-Messinian paleo-bathymetric highs in the eastern and western provinces, as well as a buried and eroded pre-Messinian shelf and Messinian detrital cone. Such buried subsalt structural relief can exert a strong control on gravity spreading because differences in salt thicknesses directly control rates and directions of gravity spreading (Gaullier, 1993). The Messinian bathymetric lows accumulated thicker salt that was more easily mobilized during Plio-Quaternary times. Messinian bathymetric highs acted as local anchor points and buttresses, opposing gravity spreading and redirecting salt movement (Loncke et al., 2002b).

Our hypothesis is supported by the following structural observations in the eastern province:

- The NNW–SSE trend of the tectonic corridor matches the local orientation of the Messinian shelf break. (Figs. 7 and 8).
- Dip lines (Fig. 8(c) for example) show that salt ridges, which grew as extensional features, become pinched off toward the NE, near the Eratosthenes Seamount. These salt ridges are locally reactivated as transpressional zones.
- The bathymetric map clearly indicates that recent movement of the sedimentary overburden within the tectonic corridor is toward the northwest (west of ESM) and toward northeast (southeast of ESM) (Fig. 7), as if the overburden were flowing around the Eratosthenes Seamount.

The following evolutionary history is proposed:

After the Messinian salinity crisis, morphology of the Nile deep-sea fan's margin was relatively uniform, except that the incised pre-Messinian shelf had a very steep eastern edge (possibly controlled by a basement fault) and the ESM was an island towering above the deep basin. Early Pliocene sediments began to be deposited above the Messinian evaporites and their coeval terrigenous deposits. Because mobile salt was present over a large area (i.e. from the base of the Messinian cone to the deep basin), the salt and overburden deformed by gravity tectonics. Upslope, the limit of normal growth faults matches pre-Messinian salt pinch-out. Where the base of the mobile salt was nearly flat, i.e. in the eastern province, gravity spreading prevailed, creating sets of polygonal minibasins, with formation of NW–SE and NE–SW grabens underlain by salt ridges. Later, the front of the deep-sea fan reached and collided against the base of the Eratosthenes Seamount, which acted as a passive buttress. The overburden in the distal part of the fan was subjected to shortening, which forced salt ridges to be squeezed (Vendeville and Nilsen, 1995) and pinched off. Because no more movement was possible toward the northeast, overall spreading direction changed, favoring a northwestward escape, where no buttress opposed seaward spreading of the overburden.

Finally, it is important to notice that physical models (sand/silicone) designed to reproduce thin-skinned tectonics in the eastern NDSF (Loncke, 2002; Loncke et al., 2002b) confirmed that the specific shape of the pre-Messinian shelf-break, a steep promontory, and the presence of a preexisting

structural high, such as the Eratosthenes Seamount, can lead to deformation patterns similar to those observed in the study area.

In the first type of experiments, we tested the influence of a passive buttress, such as the Eratosthenes Seamount (ESM), on the gravity spreading of a sedimentary lobe. The model (Fig. 12) initially included a prekinematic, sandy, circular buttress simulating the ESM. This setup is overlain by a prekinematic, silicone, mobile layer (the buttress not being totally covered by silicone), on which synkinematically prograding sandy lobes were finally deposited. These experiences evidence that the presence of a passive buttress can oppose further radial spreading of sedimentary lobes during the late stages and is responsible for strike–slip reactivations of initially extensional structures. Structures perpendicular to the buttress are reactivated in transpression, while other features remain extensional. The presence of a distal buttress also induces distal, subcircular flow patterns.

In summary, the final deformation pattern of this experiment appears similar to that of the eastern the NDSF (Fig. 12):

- (1) Polygonal depocenters, similar to the minibasins found upslope and midslope of the NDSF were created during the first stage of the experiment (radial extension).
- (2) Later, the family of N to NW trending grabens and associated underlying ridges were squeezed and reactivated in transpression, whereas faults having different orientations remained extensional. This evolution is very close to what is observed in the eastern NDSF, where NW grabens and salt ridges were pinched as they approached the ESM. Strike slip along these faults accommodated the northwestward escape of the sediment overburden. Also, extensional NW–SE structures, observed south of the ESM, seem to be close to the transtensional structures in the NDSF (giant en echelon grabens).
- (3) Finally, the distal, arcuate flow and fold pattern, and the presence of a distal bathymetric scarp in the model are similar to what is observed in the eastern NDSF.

6. Conclusions

Comparison between the structural analysis of the NDSF with results of physical experiments (Loncke, 2002; Loncke et al., 2002b) highlights the importance of structural and paleogeographic heritage on the shallow structure and evolution of thick clastic sequences deposited above a mobile substrate. And distinguishing between which structures result from thick-skinned tectonics and which from thin-skinned tectonics is crucial in the understanding of tectonically complex areas such as the eastern Mediterranean. In the NDSF, the shallow deformation pattern does not appear to reflect any regional thick-skinned tectonics, or at least not intuitively; instead, it appears to be related to the margin's Messinian morphology, which itself resulted from the interplay between both erosional and tectonic processes and the initial

delta physiography. In particular, the proximity of ESM strongly influenced post-Messinian construction of the NDSF. This topographic buttress limited and deflected the northeastward advance of Messinian evaporites. This buttressing effect, along with differences in slope gradients at the base of the salt layer has complicated deformation of the overlying Plio-Quaternary cover within a broad NNW–SSE corridor that obliquely intersects present-day bathymetry of the Nile cone.

Furthermore, the structure of the Nile cone controls not only type but also efficiency of sediment dispersal and depositional processes. Understanding the origin of this processes is important in determining confined and non-confined areas (Loncke, 2002) and in defining the hydrocarbon prospectivity of each specific area of the deep-sea fan.

Finally, study of the NDSF offers a great variety of young, salt-related structures that can be observed in bathymetry (all post-Miocene). Analysis of this delta system using modern geophysical methods provides an opportunity to characterize initial deformation on salt-bearing passive margins and to extrapolate the evolution of these early features to more mature systems. Another particularity of the NDSF is that gravity spreading and gliding processes are both clearly active within this system, giving rise to a large variety of salt-related structures from growth faults to polygonal minibasins.

The Nile margin natural example reminds us that we must recognize the importance of heritage in understanding modern fan architecture and evolution, even when the clastic wedge is decoupled from its basement by a mobile layer such as salt or shale. These results can be applied to several other deep-sea fans, including those within the western Mediterranean Sea (Gulf of Lion, Ligurian margin, etc.) or the Atlantic margins where mobile shale or salt layers are interbedded within thick sedimentary piles (North Sea, Nigeria, Angola, Gulf of Mexico, etc.).

Acknowledgements

This work was supported by several people and programs. We would like to thank especially:

- The French margin program (GDR Marges) and the CNRS/INSU Ocean group for funding this project.
- BP-Egypt for providing seismic data and 3D block first arrivals, and especially Vince Felt and Paul Boucher for their enthusiastic and constant support.
- Olivier Sardou for the processing of acoustic and bathymetric data, and Gael Lebastard for completion of the initial isopach maps.
- Peter Bentham and John Woodside for their critical review of the paper and very useful improvements.

References

- Aal, A., El Barkooky, A., Gerrits, M., Meyer, H., Schwander, M., Zaki, H., 2000. Tectonic evolution of the Eastern Mediterranean basin and its significance for hydrocarbon prospectivity in the ultradeepwater of the Nile delta. *The Leading Edge*, 1086–1102.
- Aal, A., El Barkooky, A., Gerrits, M., Meyer, H., Schwander, M., Zaki, H., 2001. Tectonic evolution of the eastern Mediterranean basin and its significance for hydrocarbon prospectivity in the ultradeepwater of the Nile delta. *GeoArabia* 6, 363–384.
- Bellaiche, G., Zitter, T., Droz, L., Gaullier, V., Mart, Y., Mascle, J., Prised II scientific parties, 1999. Le cône sous-marin profond du Nil: principaux résultats de la campagne 'Prised II' du N.O. 'l'Atalante'. *Comptes Rendus Académie Scientifique (Paris)* 329, 727–733.
- Bellaiche, G., Loncke, L., Gaullier, V., Mascle, J., Courp, T., Moreau, A., Radan, S., Sardou, O., 2001. Le cône sous-marin du Nil et son réseau de chenaux profonds: nouveaux résultats (campagne Fanil). *CRAS, Paris* 333, 399–404.
- Biju-Duval, B., Letouzey, J., Montadert, L., 1978. Variety of margins and deep basins in the Mediterranean. *AAPG Bulletin*, 293–317.
- Chaumillon, E., Mascle, J., Hoffmann, J., 1996. Deformation of the western Mediterranean Ridge: importance of Messinian evaporitic formations. *Tectonophysics* 263, 163–190.
- Cobbold, P.R., Szatmari, P., 1991. Radial gravitational gliding on passive margins. *Tectonophysics* 188, 249–289.
- Courtilot, V., Armijo, R., Tapponnier, P., 1987. Kinematics of the Sinai triple junction and a two phase model of Arabia–Africa rifting. In: Coward, M.P., Dewey, J.F., Hancock, P.L. (Eds.), *Continental Extensional Tectonics*, vol. 28. G.S.L.S. Publ., pp. 559–573.
- Cramez, C., Jackson, M.P.A., 2000. Superposed deformation straddling the continental-oceanic transition in deep-water Angola. *Marine and Petroleum Geology* 17, 1095–1109.
- Diegel, F.A., Karlo, J.F., Schuster, D.C., Shoup, R.C., Tauvers, P.R., 1995. Cenozoic structural evolution and tectono-stratigraphic framework of the northern gulf coast continental margin. In: Jackson, M.P.A., Roberts, D.G., Snelson, S. (Eds.), *Salt Tectonics: A Global Perspective American Association of Petroleum Geologists Memoir* vol. 65, pp. 109–151.
- Dolson, J.C., Boucher, P.J., Shann, M.V., 2000. Exploration potential in the offshore Mediterranean, Egypt: perspectives from the context of Egypt's future resources and business challenges. *EAGE Conference on Geology and Petroleum Geology, Malta*.
- EGPC, 1994. Nile delta and north Sinai: Fields, discoveries and hydrocarbon potentials (a comprehensive overview): Cairo, Egypt, 385 pp.
- Gaullier, V., 1993. Diapirisme salifère et dynamique sédimentaire dans le bassin Liguro-Provençal: Thèse de l'Université Pierre et Marie Curie (Paris VI), Villefranche-sur-Mer, 327 p.
- Gaullier, V., Bellaiche, G., 1996. Diapirisme liguro-provençal: les effets d'une topographie résiduelle sous le sel messinien. *Apports de la modélisation analogique. Comptes Rendus de l'Académie des Sciences de Paris* 322, 213–220.
- Gaullier, V., Vendeville, B.C., 2005. Salt tectonics driven by sediment progradation: part II—radial spreading of sedimentary lobes prograding above salt. *American Association of Petroleum Geologists Bulletin* 89, 1081–1089.
- Gaullier, V., Mart, Y., Bellaiche, G., Mascle, J., Vendeville, B., Zitter, T., Prised II scientific parties, 2000. Salt tectonics in and around the Nile Deep-Sea Fan: insights from the 'PRISMED II' cruise: from the arctic to the Mediterranean: salt, shale and igneous diapirs in and around Europe. *Geological Society* 174, 111–129 (spécial pub).
- Guiraud, R., Bosworth, W., 1999. Phanerozoic geodynamic evolution of northeastern Africa and the northwestern Arabian platform. *Tectonophysics* 315, 73–108.
- Hirsch, F., Flexer, A., Rosenfield, A., Yellin-Dror, A., 1995. Palinspastic and crustal setting of the eastern Mediterranean. *Journal of Geology* 18, 149–170.
- Huguen, C., 2001. Déformation récente à actuelle et argilo-cinèse associée au sein de la Ride Méditerranéenne: Thèse de 3ème cycle de l'université Paris 6, 260 p.
- Kempler, D., Mart, Y., Herut, B., McCoy, F., 1996. Diapiric structures in the SE Mediterranean. *Marine Geology* 134, 237–248.
- Le Pichon, X., Chamot-Rooke, N., Lallemand, S., 1995. Geodetic determination of the kinematics of central Greece with respect to Europe: Implications for eastern Mediterranean Tectonics. *Journal of Geophysical Research* 100, 12675–12690.

- Lofi, J., 2002. La Crise de Salinité Messinienne: Conséquences directes et différées sur l'évolution sédimentaire de la marge du Golfe du Lion: Thèse de doctorat de l'université de Lille I.
- Lofi, J., Rabineau, M., Gorini, C., Berne, S., Clauzon, G., De Clarens, P., Tadeu Dos Reis, A., Mountain, G.S., Ryan, W.B.F., Steckler, M.S., Fouchet, C., 2003. Plio-Quaternary prograding clinoform wedges of the western Gulf of Lion continental margin (NW Mediterranean) after the Messinian Salinity Crisis. *Marine Geology* 198, 289–317.
- Loncke, L., 2002. Le delta profond du Nil: structure et évolution depuis le messinien (Miocène terminal): Thèse de l'université Paris 6, 184 pp.
- Loncke, L., Mascle, J. Fanil scientific parties, 2004. Mud volcanoes, gas chimneys, pockmarks and mounds in the Nile deep sea fan (eastern Mediterranean): geophysical evidences. *Marine and Petroleum Geology* 21 (6), 669–689.
- Loncke, L., Gaullier, V., Bellaiche, G., Mascle, J., 2002a. Recent depositional pattern of the NDSF from echo-character mapping: interactions between turbidity currents, mass-wasting processes and tectonics. *AAPG Bulletin* 86, 1165–1186.
- Loncke, L., Vendeville, B., Gaullier, V., Mascle, J., 2002b. Contribution of physical modeling to understanding salt tectonics in the eastern Nile deep-sea fan, in 'Our Heritage-Key to Global Discovery,' Special Session: 'Pass the Salt, Please: Recent Advances in Global Salt Tectonics': AAPG Annual Convention.
- Maillard, A., Gaullier, V., Vendeville, B., Odonne, F., 2003. Influence of differential compaction above basement steps on salt tectonics in the Ligurian-Provençal basin, northwest Mediterranean. *Marine and Petroleum Geology* 20, 13–27.
- Mascle, J., Benkheilil, J., Bellaiche, G., Zitter, T., Woodside, J., Loncke, L., 2000. Marine geologic evidence for a Levantine-Sinai plate, a missing piece of the Mediterranean puzzle. *Geology* 28, 779–782.
- Mascle, J., Zitter, T., Bellaiche, G., Droz, L., Gaullier, V., Loncke, L., Pristed II scientific parties, 2001. The Nile deep-sea fan: preliminary results from a swath bathymetry survey. *Marine and Petroleum Geology* 18, 471–477.
- Mascle, J., Camera, L., Chamot-Rooke, N., Costis, C., Gaullier, V., Loncke, L., Nielsen, C., Operto, S., Ribodetti, A., Sage, F., Sallares, V., Schenini, L., 2003. New constraints on the deep structure of the eastern Mediterranean sea from new MCS seismic reflection data: EGS-AGU-EUG Joint Assembly. ISSN: 1029–7006, Abstract Number: EAE03-A-09172.
- McClusky, S., Balassanian, S., Barka, A., Demir, C., Ergintav, S., Georgiev, I., Gurkan, O., Hamburger, M., Hurst, K., Kahle, H., Kastens, K., Kekelidze, G., King, R., Kotzev, V., Lenk, O., Mahmoud, S., Mishin, A., Nadariya, M., Ouzounis, A., Paradissis, D., Peter, Y., Prilepin, M., Reilinger, R., Sanli, I., Seeger, H., Tealeb, A., Toksöz, M.N., Veis, G., 2000. GPS constraints on plate kinematics and dynamics in the eastern Mediterranean and Caucasus. *Journal of Geophysical Research* 105, 5695–5719.
- McKenzie, D., 1972. Active tectonics of the Mediterranean region. *Geophysical Journal of the Royal Astronomical Society* 30, 109–185.
- Morelli, C., 1978. Eastern Mediterranean geophysical results and implications. *Tectonophysics* 46, 333–346.
- Neev, D., 1975. Tectonic evolution of the middle east and the Levantine basin (easternmost Mediterranean). *Geology*, 683–686.
- Nilsen, K.T., Vendeville, B.C., Johansen, J.-T., 1995. Influence of regional tectonics on halokinesis in the Nordkapp basin, Barents Sea. In: Jackson, M.P.A., Roberts, D.G., Snelson, S. (Eds.), *Salt Tectonics: A Global Perspective AAPG Memoir*, vol. 65, pp. 413–436.
- Robertson, A.H.F., 1998. Tectonic significance of Eratosthenes seamount: a continental fragment in the process of collision with a subduction zone in the eastern Mediterranean (Ocean Drilling Program Leg 160). *Tectonophysics* 298, 63–82.
- Robertson, A.H.F., Kidd, R.B., Ivanov, M.K., Limonov, A.F., Woodside, J.M., Galindo-Zaldivar, J., Nieto, L., Scientific Party of the 1993 TTR-3 Cruise, 1995. Eratosthenes seamount: collisional processes in the easternmost Mediterranean in relation to the Plio-Quaternary uplift of southern Cyprus. *Terra Nova* 7, 254–264.
- Ross, D.A., Uchupi, E., 1977. The structure and sedimentary history of the southeastern Mediterranean Sea. *AAPG Bulletin* 61, 872–902.
- Rouchy, J.M., Saint-Martin, J.P., 1992. Late Miocene events in the Mediterranean as recorded by carbonate–evaporite relations. *Geology* 20, 629–632.
- Rowan, M.G., Jackson, M.P.A., Trudgill, B.D., 1999. Salt-related fault families and fault welds in the northern Gulf of Mexico. *AAPG Bulletin* 83, 1454–1484.
- Ryan, W.B.F., 1978. Messinian badlands on the southeastern margin of the Mediterranean sea. *Marine Geology* 27, 349–363.
- Ryan, W.B.F., Hsü, K.J. (Eds.), 1973. Initial Reports of the Deep-sea Drilling Project. US Government Printing Office Washington, DC, p. 1447.
- Sage, L., Letouzey, J., 1990. Convergence of the African and Eurasian plate in the eastern Mediterranean. In: Letouzey, J. (Ed.), *Petroleum and tectonics in mobile belts éditions technip*, Paris, pp. 49–68.
- Salem, R., 1976. Evolution of Eocene-Miocene sedimentation patterns in parts of northern Egypt. *AAPG Bulletin* 60, 34–64.
- Samuel, A., Kneller, B., Raslan, S., Sharp, A., Parsons, C., 2003. Prolific deep-marine slope channels of the Nile delta, Egypt. *AAPG Bulletin* 87, 541–560.
- Schreiber, E., Fox, P.J., Peterson, J.J., 1973. Compressional wave velocities in selected samples of gabbro, schist, limestone, anhydrite, gypsum and halite. In: Hsü, K.J., Ryan, W.B.F. (Eds.), *Initial reports of the Deep Sea Drilling Project*, vol. 13. US Govt. Printing Office, Washington, DC, pp. 595–598.
- Stover, S.C., Ge, S., Weimer, P., McBride, B.C., 2001. The effects of salt evolution, structural development, and fault propagation on late Mesozoic–Cenozoic oil migration: a two-dimensional fluid-flow study along a megaregional profile in the northern Gulf of Mexico Basin. *AAPG Bulletin* 85, 1945–1966.
- Trudgill, B.D., Rowan, J.C., Fiduk, P., Weimer, P.E., Gale, B.E., Korn, R.L., Phair, W.T., Gafford, G.R., Roberts, G.R., Dobbs, S.W., 1999. The Perdido fold belt, northwestern Gulf of Mexico, part 1: structural geometry, evolution and regional implications. *AAPG Bulletin* 83, 88–113.
- Vendeville, B.C., 2005. Salt tectonics driven by sediment progradation: part I—mechanics and kinematics. *American Association of Petroleum Geologists Bulletin* 89, 1071–1079.
- Vendeville, B., Cobbold, P.R., 1987. Glissements gravitaires synsédimentaires et failles normales listriques: modèles expérimentaux. *Comptes Rendus Academy Scientific (Paris)* 305, 1313–1319.
- Vendeville, B.C., Jackson, M.P.A., 1992a. The rise of diapirs during thin-skinned extension. *Marine and Petroleum Geology* 9, 331–354.
- Vendeville, B.C., Jackson, M.P.A., 1992b. The fall of diapirs during thin-skinned extension. *Marine and Petroleum Geology* 9, 354–371.
- Vendeville, B.C., Nilsen, K.T., 1995. Episodic growth of salt diapirs driven by horizontal shortening: GCSSEPM Foundation 16th Annual Research Conference, Salt, Sediment and Hydrocarbons, pp. 285–295.